Ab initio self-consistent many-body theory of polarons at all couplings

Jon Lafuente-Bartolome [1,2] Chao Lian [1,2] Weng Hong Sio [3] Idoia G. Gurtubay [4,5,6]
Asier Eiguren [4,5,6] and Feliciano Giustino [1,2,*]

[1]*Oden Institute for Computational Engineering and Sciences, The University of Texas at Austin, Austin, Texas 78712, USA*
[2]*Department of Physics, The University of Texas at Austin, Austin, Texas 78712, USA*
[3]*Institute of Applied Physics and Materials Engineering, University of Macau,*
Macao SAR 999078, People's Republic of China
[4]*Fisika Saila, University of the Basque Country UPV/EHU, 48080 Bilbao, Basque Country, Spain*
[5]*Donostia International Physics Center (DIPC), Paseo Manuel de Lardizabal 4, 20018 Donostia-San Sebastián, Spain*
[6]*EHU Quantum Center, University of the Basque Country UPV/EHU, Barrio Sarriena, s/n, 48940 Leioa, Biscay, Spain*

We present a theoretical framework to describe polarons from first principles within a many-body Green's function formalism. Starting from a general electron-phonon Hamiltonian, we derive a self-consistent Dyson equation in which the phonon-mediated self-energy is composed by two distinct terms. One term is the Fan-Migdal self-energy and describes dynamic electron-phonon processes, the other term is a contribution to the self-energy originating from the static displacements of the atomic nuclei in the polaronic ground state. The lowest-order approximation to the present theory yields the standard many-body perturbation theory approach to electron-phonon interactions in the limit of large polarons, and the *ab initio* polaron equations introduced [Sio *et al.*, Phys. Rev. B **99**, 235139 (2019); Phys. Rev. Lett. **122**, 246403 (2019)] in the limit of small polarons. A practical recipe to implement the present unifying formalism in first-principles calculations is outlined. We apply our method to the Fröhlich model, and obtain remarkably accurate polaron energies at all couplings, in line with Feynman's polaron theory and diagrammatic Monte Carlo calculations. We also recover the well-known results of Fröhlich and Pekar at weak and strong coupling, respectively. The present approach enables predictive many-body calculations of polarons in real materials at all couplings.

I. INTRODUCTION

A charge carrier propagating through a crystal may induce distortions in the lattice through the electron-phonon interaction. The quasiparticle formed by the carrier and the lattice distortion is referred to as a polaron [1–4]. The ionic displacements surrounding the carrier may lead to an increase of its effective mass, and, in the case of strong electron-phonon coupling, may ultimately form a potential well in which the polaron becomes self-trapped [5,6].

A detailed characterization of polarons in materials has been possible throughout the last decades by a combination of an array of experimental techniques [7]. Polarons have been proposed to play a crucial role in the exotic properties of several quantum materials, such as high-temperature cuprate superconductors [8], colossal magnetoresistance manganites [9], and halide perovskites [10]. In particular, the low-energy satellites observed in angle-resolved photoemission spectroscopy (ARPES) experiments are considered the hallmark of polarons in doped oxides [11–16]. It is generally accepted that polarons govern the transport [17], optical [18], and chemical properties of conducting oxides [19].

On the theoretical side, the study of polarons mostly focused on idealized models such as the Fröhlich [4,20,21] and the Holstein [22,23] models, as well as the Su-Schrieffer-Heeger model [24]. These models have provided a fertile playground for the development and application of advanced many-body techniques [25] such as variational path-integral methods [26,27], diagrammatic Monte Carlo [28,29], dynamical mean field theory [30,31], and renormalization-group approaches [32]. While these methods are of great fundamental interest, they are not directly applicable to the study of polarons in real materials.

Recent developments in density functional theory (DFT), density functional perturbation theory (DFPT), and many-body perturbation theory have opened promising new avenues to study polarons in real materials from an *ab initio* perspective [33–36]. For instance, by combining first-principles calculations with many-body Green's function techniques, it has been possible to reproduce the signatures of the electron-phonon interaction in the ARPES spectra of doped semiconductors to high accuracy [15,16,37]. However, at this level of theory, the possibility of spatial correlations between electrons and phonons is not taken into account [33] since it is generally assumed that, upon electron addition or removal, both the electron and the phonon subsystems maintain the periodicity of the original crystalline lattice.

An alternative, heuristic approach to model the formation of polarons from first principles consists of performing direct DFT calculations on supercells of insulators with an added or removed electron, and relaxing the structure to seek for

*fgiustino@oden.utexas.edu

distorted configurations which are energetically favorable with respect to the original periodic structure [38–45].

In a recent work [34,35], Sio *et al.* have formalized the DFT approach to the polaron problem, replacing supercell calculations by a set of coupled equations whose ingredients are the electron band structures, phonon dispersions, and electron-phonon matrix elements obtained from DFPT calculations in the crystal unit cell. This method established the link between model Hamiltonian and *ab initio* approaches to the polaron problem, and makes it possible to study polaron formation in materials in a systematic way.

However, the intrinsic limitations of DFT, such as the adiabatic and classical approximations for the nuclei, are naturally inherited by the method of Ref. [35]. As a consequence, this approach does not capture dynamical renormalization effects that give rise, for example, to the phonon satellites in ARPES spectra.

In this work, we generalize the theory of Ref. [35] to a many-body formalism beyond density functional theory. In particular, we present a Green's function theory of electron-phonon interactions that captures spatial correlations between lattice distortions and electrons in the many-body ground state. We find that, aside from the standard Fan-Migdal self-energy [33], one must consider an additional self-energy contribution that arises from the nonvanishing expectation value of the atomic displacements when the electron is "pinned" around a lattice site.

After presenting the general formalism, we discuss approximations that can be used to implement this methodology in existing *ab initio* codes. This analysis allows us to establish the links between our general formalism, the DFT polaron equations [34,35], and the Allen-Heine theory of band-structure renormalization [46].

As a first proof of concept, we apply our methodology to the Fröhlich model, and we benchmark our proposed approximations with respect to the all-coupling path-integral method by Feynman [26] and diagrammatic Monte Carlo calculations [28,29]. We show that our theory naturally connects the established results at weak and strong coupling limits, and predicts polaron energies with remarkably good accuracy throughout the whole range of couplings. Furthermore, as a first *ab initio* demonstration of this method, we describe in detail the computational procedure that we used to calculate the full polaronic renormalization of the band gap in LiF. The main results of this calculation and its implications in the theory of the phonon-mediated renormalization of band structures are discussed in the companion paper [47].

The paper is organized as follows. In Sec. II we develop our general formalism. In particular, we introduce the electron-phonon Hamiltonian in Sec. II A. In Sec. II B we apply Schwinger's functional derivative technique to obtain an equation of motion for the electron Green's function which can be rewritten as a Dyson equation, and identify two separate self-energy contributions. In Sec. II C we introduce an expression for the vertex function and a related approximation to simplify the equations. In Sec. II D we obtain an expression for the expectation value of the atomic displacement operator in terms of the electron density, which allows us to make the Dyson equation fully self-consistent. In Sec. III A we introduce the Lehmann representation of the electron Green's

function, which we use to derive a Schrödinger-type equation for the Dyson orbitals describing the electronic part of the polaron quasiparticle. In Sec. III B the self-energies are rewritten in terms of the polaron quasiparticle amplitudes, and in Sec. III C we present the self-consistent many-body polaron equations. In Sec. III D, an expression for the total energy in the many-body ground state of the coupled electron-phonon system is derived. In Sec. IV, we develop approximations of the many-body equations to make the formalism useful for practical *ab initio* calculations. Transparent links with the DFT polaron equations and the standard self-energies for electron-phonon coupling are established in Sec. IV B. In Sec. IV C, we outline a practical recipe to implement the lowest-order approximation to our theory in *ab initio* calculations. In Sec. V A, we apply our methodology to the Fröhlich model, and report benchmarks against the well-known weak and strong coupling limits, as well as Feynman's path-integral solution and diagrammatic Monte Carlo results. In Sec. V B, we outline the computational setup that we used to calculate polarons in LiF, as reported in the companion paper [47]. In Sec. VI we address the issue of translational invariance of the polaronic solutions, and we explain how we can "pin" the polaron at a given lattice site. In Sec. VII we summarize our key findings and we anticipate possible future developments.

II. SELF-CONSISTENT GREEN'S FUNCTION APPROACH TO POLARONS

A. Electron-phonon Hamiltonian

The starting point of our derivation is the standard Hamiltonian describing a coupled electron-phonon system [33]:

$$
\begin{aligned}
\hat{H} &= \hat{H}_e + \hat{H}_p + \hat{H}_{ep} \\
&= \sum_{n\mathbf{k}} \varepsilon_{n\mathbf{k}} \hat{c}^\dagger_{n\mathbf{k}} \hat{c}_{n\mathbf{k}} + \sum_{\mathbf{q}\nu} \hbar\omega_{\mathbf{q}\nu}(\hat{a}^\dagger_{\mathbf{q}\nu}\hat{a}_{\mathbf{q}\nu} + 1/2) \\
&\quad + N_p^{-\frac{1}{2}} \sum_{\substack{\mathbf{k},\mathbf{q} \\ mn\nu}} g_{mn\nu}(\mathbf{k},\mathbf{q}) \hat{c}^\dagger_{m\mathbf{k}+\mathbf{q}} \hat{c}_{n\mathbf{k}} (\hat{a}_{\mathbf{q}\nu} + \hat{a}^\dagger_{-\mathbf{q}\nu}),
\end{aligned}
\tag{1}
$$

where $\varepsilon_{n\mathbf{k}}$ is the single-particle eigenvalue of an electron in the band n with crystal momentum $\mathbf{k}$, $\omega_{\mathbf{q}\nu}$ is the frequency of a phonon in the branch ν with crystal momentum $\mathbf{q}$, and $\hat{c}^\dagger_{n\mathbf{k}}/\hat{c}_{n\mathbf{k}}$ ($\hat{a}^\dagger_{\mathbf{q}\nu}/\hat{a}_{\mathbf{q}\nu}$) are the associated fermionic (bosonic) creation and annihilation operators. The electron-phonon coupling matrix elements are represented by $g_{mn\nu}(\mathbf{k},\mathbf{q})$, and N_p is the number of unit cells in the periodic Born–von Kármán (BvK) supercell. To make the following derivations more compact, we introduce the complex normal coordinate operator [33]

$$
\hat{z}_{\mathbf{q}\nu} = \sqrt{\frac{\hbar}{2M_0\omega_{\mathbf{q},\nu}}} (\hat{a}_{\mathbf{q}\nu} + \hat{a}^\dagger_{-\mathbf{q}\nu}),
\tag{2}
$$

where M_0 is a reference mass. The operator $\hat{z}_{\mathbf{q}\nu}$ has dimensions of a length. We note that Eq. (1) is an effective Hamiltonian, where we assume that electron-electron interaction effects have been incorporated in the single-particle energies $\varepsilon_{n\mathbf{k}}$, so that electrons can be identified as well-defined quasiparticles in the absence of electron-phonon coupling. Moreover, phonons are described in the harmonic approximation, only linear electron-phonon coupling is retained, and the

phonon frequencies and the electron-phonon matrix elements already incorporate electronic screening at a mean-field level. In practical *ab initio* calculations, the electron energies are typically obtained via DFT or *GW* calculations [48], and phonon frequencies and electron-phonon matrix elements are obtained from DFPT calculations [49]. The use of Eq. (1) to compute most of the physical observables related to the renormalization of electrons due to the electron-phonon interaction, such as for instance temperature-dependent band structures, can be justified rigorously by starting from a more general electron-ion Hamiltonian [33]. The study of phonon renormalization requires more care [33], and it is not attempted in this work. Most model Hamiltonian approaches to the polaron problem, such as the Fröhlich [21] (see Sec. V A) or the Holstein [22,23] model, are based on further simplifications of Eq. (1).

As we discuss in detail in Sec. VI, an additional term is needed in Eq. (1) to break translational symmetry and pin the polaron at a given lattice site. In the following we omit this term for clarity since it does not alter the final results, and we return to it in Sec. VI.

B. Equation of motion for the electron Green's function

The central object in our derivation is the electron Green's function, which is defined as

$$G(\mathbf{r}t, \mathbf{r}'t') = -\frac{i}{\hbar}\langle N+1| \hat{T}\,\hat{\psi}(\mathbf{r},t)\,\hat{\psi}^\dagger(\mathbf{r}',t')\,|N+1\rangle, \quad (3)$$

where $|N+1\rangle$ represents the many-body ground state of an $(N+1)$-electron system, $\hat{T}$ is the time-ordering operator [50], and $\hat{\psi}^\dagger/\hat{\psi}$ are the electron field creation and annihilation operators. In the following we consider the electron polaron for definiteness, but our results hold unchanged for hole polarons. The field operators can be written in the single-particle basis used in Eq. (1),

$$\hat{\psi}(\mathbf{r}) = \sum_{n\mathbf{k}} \psi_{n\mathbf{k}}(\mathbf{r})\,\hat{c}_{n\mathbf{k}}, \quad (4)$$

being $\psi_{n\mathbf{k}}(\mathbf{r})$ the single-particle Bloch wave functions, so that the Green's function in the single-particle basis reads as

$$G_{n\mathbf{k},n'\mathbf{k}'}(t,t') = -\frac{i}{\hbar}\langle N+1| \hat{T}\,\hat{c}_{n\mathbf{k}}(t)\,\hat{c}^\dagger_{n'\mathbf{k}'}(t')\,|N+1\rangle. \quad (5)$$

In Eqs. (3) and (5), $|N+1\rangle$ represents the polaronic many-body ground state, which corresponds to a single electron added to semiconductor or insulator with filled valence bands and empty conduction bands, correlated with its accompanying phonon cloud. In the following, the angular brackets $\langle\ldots\rangle$ represent the expectation value of operators over the $|N+1\rangle$ state, unless otherwise specified. An important distinction from previous Green's function approaches to the polaron problem [28,29] is that in those studies the expectation value in the definition of Eq. (5) is taken over the ground state of the N-electron system, i.e., the system in absence of the extra electron. Our present choice of starting from the $|N+1\rangle$ state is useful to better connect with DFT calculations, as it will become clear shortly. We elaborate further on this point in Sec. VII.

The time dependence in the electron operators can be described within the Heisenberg picture, so that their equation of motion is given by

$$i\hbar\frac{\partial}{\partial t}\hat{c}_{n\mathbf{k}}(t) = [\hat{c}_{n\mathbf{k}}(t), \hat{H}]$$

$$= \varepsilon_{n\mathbf{k}}\hat{c}_{n\mathbf{k}}(t) + \sqrt{\frac{2\,M_0\,\omega_{\mathbf{q},\nu}}{\hbar N_p}}$$

$$\times \sum_{n'\mathbf{q}\nu} g_{nn'\nu}(\mathbf{k}-\mathbf{q},\mathbf{q})\hat{c}_{n'\mathbf{k}-\mathbf{q}}(t)\,\hat{z}_{\mathbf{q}\nu}(t), \quad (6)$$

where the anticommutation relations for the electron operators $\{\hat{c}_{n\mathbf{k}}, \hat{c}^\dagger_{n'\mathbf{k}'}\} = \delta_{n\mathbf{k},n'\mathbf{k}'}$ and $\{\hat{c}_{n\mathbf{k}}, \hat{c}_{n'\mathbf{k}'}\} = \{\hat{c}^\dagger_{n\mathbf{k}}, \hat{c}^\dagger_{n'\mathbf{k}'}\} = 0$ have been used. Combining Eqs. (5) and (6), the following equation of motion for the electron Green's function is obtained:

$$\left(i\hbar\frac{\partial}{\partial t} - \varepsilon_{n\mathbf{k}}\right)G_{n\mathbf{k},n'\mathbf{k}'}(t,t')$$

$$= \delta(t-t')\,\delta_{n\mathbf{k},n'\mathbf{k}'} - \frac{i}{\hbar}N_p^{-\frac{1}{2}}\sum_{n''\mathbf{q}\nu} g_{nn''\nu}(\mathbf{k}-\mathbf{q},\mathbf{q})$$

$$\times \sqrt{\frac{2\,M_0\,\omega_{\mathbf{q},\nu}}{\hbar}}\langle\, \hat{T}\,\hat{z}_{\mathbf{q}\nu}(t)\,\hat{c}_{n''\mathbf{k}-\mathbf{q}}(t)\,\hat{c}^\dagger_{n'\mathbf{k}'}(t')\,\rangle. \quad (7)$$

In order to deal with the last term of Eq. (7), we proceed with Schwinger's functional derivative technique [51,52]. The main idea is to add an external source term that couples to the normal mode coordinates via

$$\hat{H}_{\text{ext}}(t) = \sum_{\mathbf{q}\nu} F_{\mathbf{q}\nu}(t)\,\hat{z}_{\mathbf{q}\nu}(t). \quad (8)$$

This term will be set to zero at the end of the derivation, but it is instrumental to obtain a set of self-consistent equations for the electron Green's function by taking functional derivatives with respect to the fictitious forces $F_{\mathbf{q}\nu}(t)$. Furthermore, this term is needed to break translational symmetry and pin the polaron around a lattice site (see Sec. VI). The Schwinger's functional derivative technique has proven very successful in electronic structure theory, and is at the heart of all modern developments in the *GW* method [53–55].

We rewrite Eq. (7) using the following functional identity, first derived in Ref. [52] and employed extensively in Refs. [56,57]:

$$\frac{\delta\langle\, \hat{T}\,\hat{O}_1(t_1)\hat{O}_2(t_2)\ldots\rangle}{\delta F_{\mathbf{q}\nu}(t)} = -\frac{i}{\hbar}\langle\, \hat{T}\,\hat{z}_{\mathbf{q}\nu}(t)\,\hat{O}_1(t_1)\hat{O}_2(t_2)\ldots\rangle$$

$$+ \frac{i}{\hbar}\langle\hat{z}_{\mathbf{q}\nu}(t)\rangle\langle\, \hat{T}\,\hat{O}_1(t_1)\hat{O}_2(t_2)\ldots\rangle. \quad (9)$$

Here, $\hat{O}$ represents a generic many-body operator. Using this expression, Eq. (7) becomes

$$\left(i\hbar\frac{\partial}{\partial t} - \varepsilon_{n\mathbf{k}}\right)G_{n\mathbf{k},n'\mathbf{k}'}(t,t')$$

$$= \delta(t-t')\,\delta_{n\mathbf{k},n'\mathbf{k}'} + N_p^{-\frac{1}{2}}\sum_{n''\mathbf{q}\nu} g_{nn''\nu}(\mathbf{k}-\mathbf{q},\mathbf{q})$$

$$\times \sqrt{\frac{2\,M_0\,\omega_{\mathbf{q},\nu}}{\hbar}}\left(i\hbar\frac{\delta}{\delta F_{\mathbf{q}\nu}(t)} + \langle\hat{z}_{\mathbf{q}\nu}(t)\rangle\right)G_{n''\mathbf{k}-\mathbf{q},n'\mathbf{k}'}(t,t'). \quad (10)$$

To eliminate the dependence on $F_{\mathbf{q}\nu}(t)$, we first rewrite the functional derivative in the last term in terms of the inverse of the Green's function [58]

$$\frac{\delta G_{n\mathbf{k},n'\mathbf{k}'}(t,t')}{\delta F_{\mathbf{q}\nu}(t)} = -\int dt'' dt''' \sum_{\substack{n''\mathbf{k}'' \\ n'''\mathbf{k}'''}} G_{n\mathbf{k},n''\mathbf{k}''}(t,t'') \frac{\delta G^{-1}_{n''\mathbf{k}'',n'''\mathbf{k}'''}(t'',t''')}{\delta F_{\mathbf{q}\nu}(t)} G_{n'''\mathbf{k}''',n'\mathbf{k}'}(t''',t'), \tag{11}$$

and then we apply the following functional chain rule [58]:

$$\frac{\delta G^{-1}_{n\mathbf{k},n'\mathbf{k}'}(t,t')}{\delta F_{\mathbf{q}\nu}(t'')} = \int dt''' \sum_{\mathbf{q}'\nu'} \frac{\delta G^{-1}_{n\mathbf{k},n'\mathbf{k}'}(t,t')}{\delta\langle\hat{z}_{\mathbf{q}'\nu'}(t''')\rangle} \frac{\delta\langle\hat{z}_{\mathbf{q}'\nu'}(t''')\rangle}{\delta F_{\mathbf{q}\nu}(t'')}. \tag{12}$$

The last term on the right-hand side can be identified with the phonon Green's function, which is given by

$$D_{\mathbf{q}'\nu',\mathbf{q}\nu}(t',t) = -i\sqrt{\frac{2M_0\omega_{\mathbf{q}\nu}}{\hbar}}\sqrt{\frac{2M_0\omega_{\mathbf{q}'\nu'}}{\hbar}}\langle\hat{T}[\hat{z}_{\mathbf{q}'\nu'}(t') - \langle\hat{z}_{\mathbf{q}'\nu'}(t')\rangle][\hat{z}_{\mathbf{q}\nu}(t) - \langle\hat{z}_{\mathbf{q}\nu}(t)\rangle]\rangle. \tag{13}$$

In fact, by using this definition inside Eq. (9), we find

$$\frac{\delta\langle\hat{z}_{\mathbf{q}\nu}(t)\rangle}{\delta F_{\mathbf{q}'\nu'}(t')} = \frac{1}{\sqrt{2M_0\omega_{\mathbf{q}\nu}}}\frac{1}{\sqrt{2M_0\omega_{\mathbf{q}'\nu'}}}D_{\mathbf{q}\nu,\mathbf{q}'\nu'}(t,t'). \tag{14}$$

Now we define the vertex function as

$$\Gamma_{n\mathbf{k},n'\mathbf{k}',\nu\mathbf{q}}(t,t',t'') = -\sqrt{\frac{\hbar}{2M_0\omega_{\mathbf{q}\nu}}}\frac{\delta G^{-1}_{n\mathbf{k},n'\mathbf{k}'}(t,t')}{\delta\langle\hat{z}_{\mathbf{q}\nu}(t'')\rangle}, \tag{15}$$

and we write the noninteracting Green's function as

$$(G^0)^{-1}_{n\mathbf{k},n'\mathbf{k}'}(t,t') = \left(i\hbar\frac{\partial}{\partial t} - \varepsilon_{n\mathbf{k}}\right)\delta(t-t')\delta_{n\mathbf{k},n'\mathbf{k}'}. \tag{16}$$

Using the last two relations together with Eqs. (11)–(14), we can rewrite Eq. (10) as a Dyson equation:

$$\int dt''\sum_{n''\mathbf{k}''}\left[(G^0)^{-1}_{n\mathbf{k},n''\mathbf{k}''}(t,t'') - \Sigma^{P}_{n\mathbf{k},n''\mathbf{k}''}(t,t'') - \Sigma^{FM}_{n\mathbf{k},n''\mathbf{k}''}(t,t'')\right]G_{n''\mathbf{k}'',n'\mathbf{k}'}(t'',t') = \delta(t-t')\delta_{n\mathbf{k},n'\mathbf{k}'}, \tag{17}$$

where the self-energies Σ^{P} and Σ^{FM} are defined as follows:

$$\Sigma^{FM}_{n\mathbf{k},n'\mathbf{k}'}(t,t') = iN_p^{-1/2}\int dt'' dt'''\sum_{n''\mathbf{k}''}\sum_{n'''\mathbf{k}'''}\sum_{\nu\nu'\mathbf{q}'} g_{nn''\nu}(\mathbf{k}'',\mathbf{k}-\mathbf{k}'')G_{n''\mathbf{k}'',n'''\mathbf{k}'''}(t,t''')$$

$$\times \Gamma_{n'''\mathbf{k}''',n'\mathbf{k}',\mathbf{q}'\nu'}(t''',t',t'')D_{\mathbf{q}'\nu',\mathbf{k}-\mathbf{k}''\nu}(t'',t), \tag{18}$$

$$\Sigma^{P}_{n\mathbf{k},n'\mathbf{k}'}(t,t') = N_p^{-1/2}\sum_{\nu}\sqrt{\frac{2M_0\omega_{\mathbf{k}-\mathbf{k}',\nu}}{\hbar}}g_{nn'\nu}(\mathbf{k}',\mathbf{k}-\mathbf{k}')\langle\hat{z}_{\mathbf{k}-\mathbf{k}'\nu}(t)\rangle\delta(t-t'), \tag{19}$$

and the superscripts "FM" and "P" stand for Fan-Migdal and polaronic, respectively. Note that $(G^0)^{-1}_{n\mathbf{k},n'\mathbf{k}'}(t,t')$ and $\Sigma_{n\mathbf{k},n'\mathbf{k}'}(t,t')$ have units of energy divided by time.

A diagrammatic representation of the self-energy Σ^{FM} in Eq. (18) is given in Fig. 1(a). In Sec. IV A we show how, using a standard approximation for the vertex Γ, we can identify Σ^{FM} in Eq. (18) with the standard Fan-Migdal (FM) self-energy [33]. This self-energy has been key to interpret the spectral kinks and satellites observed in photoemission experiments [11,15,37,59,60], and leads to the Allen-Heine [46] theory of band-structure renormalization including its nonadiabatic generalizations [61–69] upon performing the pertinent approximations (see, e.g., Ref. [33]).

To the best of our knowledge, the self-energy Σ^{P} in Eq. (19) appeared in Refs. [57,70], but the connection to polaron formation was not appreciated. This self-energy

accounts for the static renormalization of electron energies due to localization effects. In fact, as we show below, this self-energy reproduces the Pekar solution to the Fröhlich polaron problem in the limit of strong coupling [6].

C. Vertex function

In order to obtain a closed self-consistent set of equations, we need to express the vertex function Γ in Eq. (15) in terms of the electron Green's function. To this aim, we first invert the Dyson equation in Eq. (17),

$$G^{-1}_{n\mathbf{k},n'\mathbf{k}'}(t,t') = (G^0)^{-1}_{n\mathbf{k},n'\mathbf{k}'}(t,t') - \Sigma_{n\mathbf{k},n'\mathbf{k}'}(t,t'), \tag{20}$$

so that we can take the functional derivatives for each term separately. In the remainder of this section we use numbered indices for convenience.
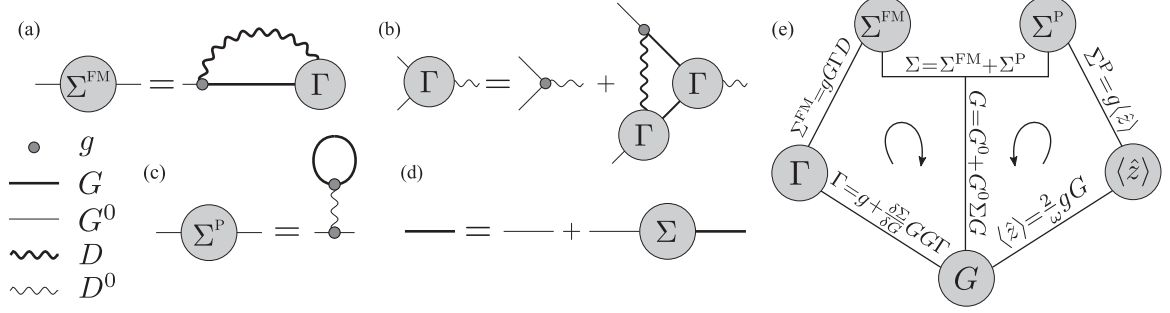
FIG. 1. Diagrammatic representation of the self-consistent Green's function theory of polarons. Legends for the different parts of the diagrams are given in the lower left corner. (a) Fan-Migdal self-energy in Eq. (18). (b) Self-consistent definition of the vertex function in Eq. (24). (c) Polaronic self-energy in Eq. (33). (d) Dyson equation (17). (e) Schematic representation of the self-consistent solution of Eqs. (17), (18), (24), and (33).

From Eq. (16), we see that $\delta(G^0)^{-1}/\delta\langle\hat{z}\rangle = 0$. The functional derivatives of Σ^P and Σ^{FM} are obtained as follows. For the polaronic self-energy in Eq. (19), we find

$$\frac{\delta\Sigma^P_{n_1\mathbf{k}_1,n_2\mathbf{k}_2}(t_1,t_2)}{\delta\langle\hat{z}_{\mathbf{q}_3\nu_3}(t_3)\rangle} = \delta(t_1-t_2)\delta(t_1-t_3)\delta_{\mathbf{q}_3,\mathbf{k}_1-\mathbf{k}_2}$$

$$\times N_p^{-\frac{1}{2}}\sqrt{\frac{2M_0\,\omega_{\mathbf{q}_3,\nu}}{\hbar}}\,g_{n_1n_2\nu_3}(\mathbf{k}_2,\mathbf{q}_3). \quad (21)$$

For the FM self-energy, we apply the chain rule as in Eq. (12),

$$\frac{\delta\Sigma^{FM}_{n_1\mathbf{k}_1,n_2\mathbf{k}_2}(t_1,t_2)}{\delta\langle\hat{z}_{\mathbf{q}_3\nu_3}(t_3)\rangle} = \int dt_4 dt_5 \sum_{\substack{n_4\mathbf{k}_4\\n_5\mathbf{k}_5}}\frac{\delta\Sigma^{FM}_{n_1\mathbf{k}_1,n_2\mathbf{k}_2}(t_1,t_2)}{\delta G_{n_4\mathbf{k}_4,n_5\mathbf{k}_5}(t_4,t_5)}$$

$$\times \frac{\delta G_{n_4\mathbf{k}_4,n_5\mathbf{k}_5}(t_4,t_5)}{\delta\langle\hat{z}_{\mathbf{q}_3\nu_3}(t_3)\rangle}. \quad (22)$$

This expression can be simplified using G^{-1} as in Eq. (11):

$$\frac{\delta G_{n_4\mathbf{k}_4,n_5\mathbf{k}_5}(t_4,t_5)}{\delta\langle\hat{z}_{\mathbf{q}_3\nu_3}(t_3)\rangle} = -\int dt_6 dt_7 \sum_{\substack{n_6\mathbf{k}_6\\n_7\mathbf{k}_7}} G_{n_4\mathbf{k}_4,n_6\mathbf{k}_6}(t_4,t_6)$$

$$\times \frac{\delta G^{-1}_{n_6\mathbf{k}_6,n_7\mathbf{k}_7}(t_6,t_7)}{\delta\langle\hat{z}_{\mathbf{q}_3\nu_3}(t_3)\rangle}G_{n_7\mathbf{k}_7,n_5\mathbf{k}_5}(t_7,t_5). \quad (23)$$

In this expression we recognize the vertex function appearing in the integrand, in the form of Eq. (15). Combining Eqs. (15) and (20)–(23), we arrive at the following self-consistent expression for the vertex function:

$$\Gamma_{n_1\mathbf{k}_1,n_2\mathbf{k}_2,\nu_3\mathbf{q}_3}(t_1,t_2,t_3) = \delta(t_1-t_2)\,\delta(t_1-t_3)\,\delta_{\mathbf{q}_3,\mathbf{k}_1-\mathbf{k}_2}\,N_p^{-\frac{1}{2}}\,g_{n_1n_2\nu_3}(\mathbf{k}_2,\mathbf{q}_3)$$

$$+ \int dt_4 dt_5 dt_6 dt_7 \sum_{\substack{n_4\mathbf{k}_4\\n_5\mathbf{k}_5\\n_6\mathbf{k}_6\\n_7\mathbf{k}_7}}\frac{\delta\Sigma^{FM}_{n_1\mathbf{k}_1,n_2\mathbf{k}_2}(t_1,t_2)}{\delta G_{n_4\mathbf{k}_4,n_5\mathbf{k}_5}(t_4,t_5)}G_{n_4\mathbf{k}_4,n_6\mathbf{k}_6}(t_4,t_6)G_{n_7\mathbf{k}_7,n_5\mathbf{k}_5}(t_7,t_5)\Gamma_{n_6\mathbf{k}_6,n_7\mathbf{k}_7,\nu_3\mathbf{q}_3}(t_6,t_7,t_3). \quad (24)$$

A diagrammatic representation of Eq. (24) is given in Fig. 1(b).

D. Atomic displacements and polaronic self-energy

The expectation value of the normal-mode operator that appears in the polaronic self-energy Σ^P can be expressed as [33]

$$\langle\hat{z}_{\mathbf{q}\nu}\rangle = N_p^{-\frac{1}{2}}\sum_{\kappa\alpha p}e^{-i\mathbf{q}\cdot\mathbf{R}_p}\sqrt{\frac{M_\kappa}{M_0}}e^*_{\kappa\alpha,\nu}(\mathbf{q})\langle\Delta\hat{\tau}_{\kappa\alpha p}\rangle, \quad (25)$$

where $\Delta\hat{\tau}_{\kappa\alpha p}$ represents the operator for the displacement of the nucleus κ in the unit cell p along the Cartesian direction α, $e_{\kappa\alpha,\nu}(\mathbf{q})$ is the polarization vector of the phonon branch ν at momentum $\mathbf{q}$, M_κ is the mass of the nucleus κ, M_0 is a reference mass (e.g., the proton mass), and $\mathbf{R}_p$ is the lattice vector of the unit cell p. Equations (17), (19), and (25) show that, if

in the polaron ground state the atoms are displaced from their equilibrium sites, then there is an additional self-energy term to be added to the standard FM self-energy contribution. In the following, we show that the value of the atomic displacements is determined by the ground-state electron density, which in turn can be written self-consistently in terms of the renormalized electron Green's function G.

In order to obtain an explicit expression for $\langle\Delta\hat{\tau}_{\kappa\alpha p}\rangle$, it is convenient to rewrite the electron-phonon interaction term of the Hamiltonian in Eq. (1) as [33]

$$\hat{H}_{ep} = \int d\mathbf{r}\sum_{\kappa\alpha p}\frac{\partial V^0_{tot}(\mathbf{r})}{\partial\tau_{\kappa\alpha p}}\hat{n}_e(\mathbf{r})\,\Delta\hat{\tau}_{\kappa\alpha p}, \quad (26)$$

where $V^0_{tot}(\mathbf{r})$ is the total (electronic plus ionic) electrostatic potential in the absence of the excess electron, and $\hat{n}_e(\mathbf{r}) = \hat{\psi}^\dagger(\mathbf{r})\hat{\psi}(\mathbf{r})$ is the electron density operator. Similarly, the phonon term of the Hamiltonian in Eq. (1) can be rewritten

as [33]

$$\hat{H}_{\text{p}} = -\sum_{\kappa\alpha p} \frac{\hbar^2}{2M_\kappa} \frac{\partial^2}{\partial \tau_{\kappa\alpha p}^2} + \frac{1}{2} \sum_{\substack{\kappa\alpha p \\ \kappa'\alpha'p'}} C_{\kappa\alpha p, \kappa'\alpha'p'} \Delta\hat{\tau}_{\kappa\alpha p} \Delta\hat{\tau}_{\kappa'\alpha'p'},$$

(27)

where $C_{\kappa\alpha p, \kappa'\alpha'p'}$ is the matrix of the interatomic force constants.

From Eqs. (26) and (27), an equation of motion for the displacement operator resembling Newton's equation can be obtained:

$$\frac{d^2}{dt^2} \Delta\hat{\tau}_{\kappa\alpha p}(t) = -\frac{1}{\hbar^2} [[\Delta\hat{\tau}_{\kappa\alpha p}(t), \hat{H}], \hat{H}].$$

(28)

Using the commutation relations $[\Delta\hat{\tau}_{\kappa\alpha p}, \Delta\hat{\tau}_{\kappa'\alpha'p'}] = [\hat{p}_{\kappa\alpha p}, \hat{p}_{\kappa'\alpha'p'}] = 0$ and $[\Delta\hat{\tau}_{\kappa\alpha p}, \hat{p}_{\kappa'\alpha'p'}] = i\hbar\,\delta_{\kappa\alpha p, \kappa'\alpha'p'}$, where $\hat{p}_{\kappa\alpha p} = -i\hbar\,\partial/\partial\tau_{\kappa\alpha p}$, and taking the expectation value on the polaron ground state, we are left with a second-order nonhomogeneous differential equation for $\langle\Delta\hat{\tau}_{\kappa\alpha p}\rangle$:

$$\frac{d^2}{dt^2} \langle\Delta\hat{\tau}_{\kappa\alpha p}(t)\rangle = -\sum_{\kappa'\alpha'p'} \frac{C_{\kappa\alpha p, \kappa'\alpha'p'}}{M_\kappa} \langle\Delta\hat{\tau}_{\kappa'\alpha'p'}(t)\rangle$$
$$- \frac{1}{M_\kappa} \int d\mathbf{r} \frac{\partial V_{\text{tot}}^0(\mathbf{r})}{\partial\tau_{\kappa\alpha p}} n_{\text{e}}(\mathbf{r}),$$

(29)

where $n_{\text{e}}(\mathbf{r}) = \langle\hat{n}_{\text{e}}(\mathbf{r}, t)\rangle$ is the expectation value of the density operator on the ground state, which is stationary. The first line of Eq. (29) serves as the complementary homogeneous equation, whose solution is given by a linear combination of normal vibrational modes

$$\langle\Delta\hat{\tau}_{\kappa\alpha p}^{\text{hom}}(t)\rangle = \sum_{\mathbf{q}\nu} u_{\mathbf{q}\nu} \sqrt{\frac{M_0}{M_\kappa}} e_{\kappa\alpha,\nu}(\mathbf{q}) e^{i\mathbf{q}\cdot\mathbf{R}_p} e^{-i\omega_{\mathbf{q}\nu}t},$$

(30)

where the constants $u_{\mathbf{q}\nu}$ have to be determined by the initial conditions. In the absence of external fields and in the thermodynamic limit, these should yield a thermalized distribution of the atomic displacements. For a finite supercell, one could use, for example, the ZG displacements introduced in Refs. [71,72] as an initial configuration. In a more refined treatment, these initial thermal displacements could be obtained starting from a formulation of the problem using the Keldysh contour extended to include a vertical leg in the complex plane [73,74]. This nonequilibrium formulation of the polaron problem is potentially promising and should be explored in future work. A particular solution of Eq. (29) is given by

$$\langle\Delta\hat{\tau}_{\kappa\alpha p}\rangle = -\sum_{\kappa'\alpha'p'} C_{\kappa\alpha p, \kappa'\alpha'p'}^{-1} \int d\mathbf{r} \frac{\partial V_{\text{tot}}^0(\mathbf{r})}{\partial\tau_{\kappa'\alpha'p'}} n_{\text{e}}(\mathbf{r}).$$

(31)

The general solution of Eq. (29) is given by the sum of Eqs. (30) and (31). However, we note that the time average of Eq. (30) vanishes. Furthermore, in the presence of anharmonic phonon-phonon couplings, which are not included in our Hamiltonian (1), the amplitude of the fluctuations in Eq. (30) must decay with a characteristic phonon lifetime. Since we are interested in equilibrium properties of the polaronic state, we neglect the fluctuations in Eq. (30), and focus on the static term in Eq. (31) as the average of the atomic displacement operator.

The expectation value of the displacement operator in Eq. (31) can be linked with the electron Green's function introduced in Sec. II B via the standard relation [56]

$$\langle\hat{n}_{\text{e}}(\mathbf{r})\rangle = -i\hbar\,G(\mathbf{r}t, \mathbf{r}t^+)$$
$$= -\frac{\hbar}{\pi} \int_{-\infty}^{\mu} d\omega\,\text{Im}[G(\mathbf{r}, \mathbf{r}; \omega)],$$

(32)

where μ is the chemical potential. This relation derives directly from the definition of G in Eq. (3).

Combining Eqs. (3)–(5), (19), (25), (31), and (32), we find the following self-consistent expression for the polaronic self-energy:

$$\Sigma_{n\mathbf{k}, n'\mathbf{k}'}^{\text{P}}(t, t') = -\delta(t - t') \frac{2}{N_p} \sum_{n''n'''\mathbf{k}''\nu} \frac{g_{nn'\nu}(\mathbf{k}', \mathbf{k} - \mathbf{k}')}{\hbar\omega_{\mathbf{k}-\mathbf{k}',\nu}}$$
$$\times [-i\hbar\,G_{n'''\mathbf{k}''+\mathbf{k}-\mathbf{k}', n''\mathbf{k}''}(t, t^+)]$$
$$\times g_{n'''n''\nu}^*(\mathbf{k}'', \mathbf{k} - \mathbf{k}').$$

(33)

A diagrammatic representation of Eq. (33) is given in Fig. 1(c), where we can recognize that the polaronic self-energy shows a tadpole structure similar to the Hartree self-energy term found in the electron-electron problem [70,75].

Equations (18), (24), and (33), together with the Dyson equation given in Eq. (17) and shown in Fig. 1(d), form a closed set of self-consistent equations, similar to the Hedin equations in the electron-electron problem [56,76]. A graphical representation of the interdependence of the different elements is shown in Fig. 1(e).

Calculations of polarons using these equations are beyond the reach of current computational methods. In the following sections we introduce standard approximations that make this problem tractable and amenable to *ab initio* calculations.

III. MANY-BODY POLARON EQUATIONS

A. Lehmann representation in the polaron problem

In this section we move from the Green's function to Dyson orbitals using the Lehmann representation. To begin with, we recall that the Fourier transform of the Green's function can be written in the Lehmann representation as [50]

$$G(\mathbf{r}, \mathbf{r}'; \omega) = \sum_s \frac{f_s(\mathbf{r}) f_s^*(\mathbf{r}')}{\hbar\omega - [\varepsilon_s + i\eta\,\text{sgn}(\mu - \varepsilon_s)]},$$

(34)

where $\eta \to 0^+$, the functions f_s are Dyson orbitals, and the energies ε_s are electron addition and removal energies. We define these quantities below. Since our reference state is the $(N+1)$-electron system, our notation for the Lehmann representation differs slightly from the conventional notation. In Eq. (34), the electron addition and removal energies are defined as

$$\varepsilon_s = E_{N+2,s} - E_{N+1} \quad \text{for } \varepsilon_s \geqslant \mu,$$

(35)

$$\varepsilon_s = E_{N+1} - E_{N,s} \quad \text{for } \varepsilon_s < \mu,$$

(36)

where $E_{N+1\pm1,s}$ is the energy corresponding to the $|N+1\pm1, s\rangle$ many-body eigenstate of the Hamiltonian in Eq. (1), E_{N+1} is the ground-state energy of the reference

$(N+1)$-particle system, and $\mu = \frac{\partial E_{N+1}}{\partial N}$. The Dyson orbitals f_s are given by [56]

$$f_s(\mathbf{r}) = \langle N+1 \mid \hat{\psi}(\mathbf{r}) \mid N+2, s \rangle \quad \text{for } \varepsilon_s \geqslant \mu, \quad (37)$$

$$f_s(\mathbf{r}) = \langle N, s \mid \hat{\psi}(\mathbf{r}) \mid N+1 \rangle \quad \text{for } \varepsilon_s < \mu. \quad (38)$$

The physical interpretation of these Dyson orbitals within the polaron problem is discussed below. Given that we are mainly interested in occupied polaron states, we will focus on the case $\varepsilon_s < \mu$. A similar reasoning holds for the case $\varepsilon_s \geqslant \mu$.

In Eq. (38), $f_s(\mathbf{r})$ gives the probability amplitude for the state $\hat{\psi}^\dagger(\mathbf{r})|N, s\rangle$ to be contained in the reference $|N+1\rangle$ ground state. The state $\hat{\psi}^\dagger(\mathbf{r})|N, s\rangle$ is a quantum state (not necessarily an eigenstate) with $N+1$ electrons, which is obtained by adding an electron at position $\mathbf{r}$ to the excited eigenstate $|N, s\rangle$ of the N-electron system.

Now, the many-body eigenstates $|N+1\rangle$ and $|N, s\rangle$ correspond to correlated electron-phonon states. Since $\hat{\psi}(\mathbf{r})$ acts purely on the electronic component of these states, for $f_s(\mathbf{r})$ to be sizable, the phonon part of $|N, s\rangle$ has to overlap significantly with the phonon part in the $|N+1\rangle$ ground state. Thus, if $|N+1\rangle$ corresponds to a localized polaron configuration in which the atoms are displaced with respect to the periodic lattice, the first electron addition and removal energy ε_s with a sizable Dyson amplitude corresponds to the removal energy of the extra electron while the ions remain frozen in the distorted structure. Other $|N, s\rangle$ states with different atomic configurations still having vibrational wave functions nonorthogonal to $|N+1\rangle$ will yield finite but exponentially small Dyson amplitudes, and will not be considered in the following (this is best seen by considering the coherent-state approximation of Sec. III D). The first $|N, s\rangle$ state yielding a sizable $f_s(\mathbf{r})$ differs from the ground state of the N-electron system due to the lattice distortion. In order to reach the N-electron ground state, the energy released by the distorted lattice upon relaxation must be accounted for. A schematic representation of this process, and its relation to the polaron formation energy (which will be discussed in Sec. III D), is given in Fig. 2. The Dyson orbital for the lowest-energy state of the N-particle system, say $f_{s_{\min}}(\mathbf{r})$, has a simple physical interpretation if we approximate the exact many-body state $|N, s_{\min}\rangle$ by a single Slater determinant. Indeed, in this case, all valence electronic states must be occupied, and $f_{s_{\min}}(\mathbf{r})$ constitutes the lowest-energy single-particle wave function in the conduction manifold. Therefore, this Dyson orbital represents the electronic part of the polaron wave function.

B. Self-energies in terms of the polaron quasiparticle amplitudes

Following Ref. [35], we proceed by expanding the Dyson orbitals in a single-particle basis:

$$f_s(\mathbf{r}) = N_p^{-1/2} \sum_{n\mathbf{k}} A_{n\mathbf{k}}^s \, \psi_{n\mathbf{k}}(\mathbf{r}). \quad (39)$$

In the following we refer to the coefficients $A_{n\mathbf{k}}^s$ as the polaron quasiparticle amplitudes. After combining Eqs. (25), (31), (32), (34), and (39), and using the standard relations between the electron-phonon matrix elements, interatomic force constant matrix, and vibrational eigenmodes [33,35], we can express the expectation values of the normal-mode
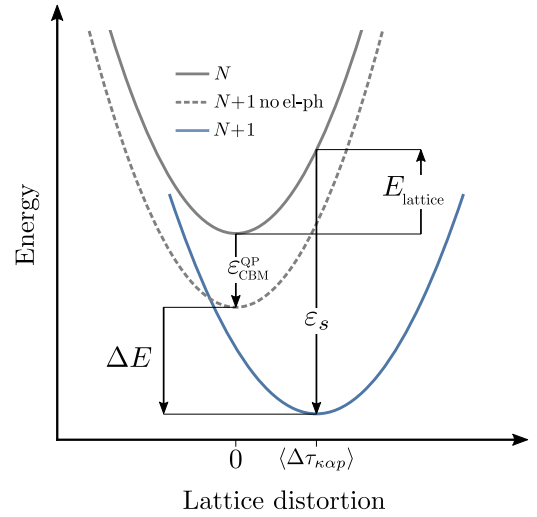

FIG. 2. Schematic representation of the different energies involved in the polaron formation process. The solid gray line represents the original periodic N-electron system, and the solid blue line represents the $(N+1)$-electron system for which a distorted polaron configuration is the ground state in the presence of a pinning potential (cf. Sec. VI). The dashed gray line represents a fictitious $(N+1)$-electron system in which an electron with no phonon-mediated renormalization has been added to the conduction band minimum ($\varepsilon_{\text{CBM}}^{\text{QP}}$). The excitation energy from the $(N+1)$-electron ground state to the distorted N-electron state is the electron addition or removal energy ε_s. The energy released by the relaxation of the lattice back to the periodic configuration is represented by E_{lattice}. The polaron formation energy, that is the energy gained by the system when a delocalized electronic state becomes localized in a polaronic state, is represented by ΔE.

coordinates as

$$\langle \hat{z}_{\mathbf{q}\nu} \rangle = -2N_p^{-3/2} \sqrt{\frac{\hbar}{2M_0 \omega_{\mathbf{q}\nu}}}$$

$$\times \sum_s \sum_{\mathbf{k}nn'}^{\varepsilon_s < \mu} A_{n'\mathbf{k}+\mathbf{q}}^s \frac{g_{n'n\nu}^*(\mathbf{k},\mathbf{q})}{\hbar\omega_{\mathbf{q}\nu}} (A_{n\mathbf{k}}^s)^*. \quad (40)$$

Using this expression inside Eq. (19), and transforming to the frequency domain, we obtain the polaronic self-energy in terms of the polaron quasiparticle amplitudes:

$$\Sigma_{n\mathbf{k},n'\mathbf{k}'}^{\text{P}}(\omega) = -\frac{2}{N_p^2} \sum_\nu g_{nn'\nu}(\mathbf{k}',\mathbf{k}-\mathbf{k}')$$

$$\times \sum_s \sum_{\mathbf{k}''mm'}^{\varepsilon_s < \mu} A_{m'\mathbf{k}''+\mathbf{k}-\mathbf{k}'}^s \frac{g_{m'm\nu}^*(\mathbf{k}'',\mathbf{k}-\mathbf{k}')}{\hbar\omega_{\mathbf{k}-\mathbf{k}'\nu}} (A_{m\mathbf{k}''}^s)^*. \quad (41)$$

We proceed similarly for the FM self-energy. In view of practical calculations, we approximate the vertex function in Eq. (24) by retaining only the term in the first line [57,77]. This is the well-known Migdal approximation, and is a standard procedure in the electron-phonon literature [33,78]. With this approximation, the FM self-energy in Eq. (18)

becomes

$$\Sigma^{\text{FM}}_{n\mathbf{k},n'\mathbf{k}'}(t,t') = \frac{i}{N_p} \sum_{\substack{m\mathbf{k}''\nu \\ m'\mathbf{k}'''\nu'}} g^*_{mn\nu}(\mathbf{k},\mathbf{k}''-\mathbf{k})\, g_{m'n'\nu'}(\mathbf{k}',\mathbf{k}'''-\mathbf{k}')\, G_{m\mathbf{k}'',m'\mathbf{k}'''}(t,t')\, D_{\mathbf{k}''-\mathbf{k}\nu,\mathbf{k}'''-\mathbf{k}'\nu'}(t,t'),$$ (42)

having used the relation $g_{nn'\nu}(\mathbf{k}',\mathbf{k}-\mathbf{k}') = g^*_{n'n\nu}(\mathbf{k},\mathbf{k}'-\mathbf{k})$ to achieve a compact expression. Along similar lines as in Eq. (41), we write the FM self-energy in the frequency domain and in terms of the quasiparticle amplitudes, by combining Eqs. (34), (39), and (42):

$$\Sigma^{\text{FM}}_{n\mathbf{k},n'\mathbf{k}'}(\omega) = \frac{i}{N_p^2} \sum_{\substack{n''\mathbf{k}''\nu \\ n'''\mathbf{k}'''\nu'}} g^*_{n''n\nu}(\mathbf{k},\mathbf{k}''-\mathbf{k})\, g_{n'''n'\nu'}(\mathbf{k}',\mathbf{k}'''-\mathbf{k}') \int \frac{d\omega'}{2\pi} \sum_s \frac{A^s_{n''\mathbf{k}''}(A^s_{n'''\mathbf{k}'''})^* D_{\mathbf{k}''-\mathbf{k}\nu,\mathbf{k}'''-\mathbf{k}'\nu'}(\omega')}{\hbar\omega - \hbar\omega' - \varepsilon_s - i\eta\, \text{sgn}(\mu-\varepsilon_s)}.$$ (43)

In order to proceed further, we approximate the interacting phonon Green's function by its adiabatic counterpart [33]:

$$D^0_{\mathbf{q}\nu,\mathbf{q}'\nu'}(\omega) = \left[\frac{1}{\omega - \omega_{\mathbf{q}\nu} + i\eta} - \frac{1}{\omega + \omega_{\mathbf{q}\nu} - i\eta} \right] \delta_{\mathbf{q}\mathbf{q}'} \delta_{\nu\nu'}.$$ (44)

This approximation is well justified and usually very accurate because the vibrational frequencies are obtained from DFPT calculations. By inserting Eq. (44) inside Eq. (43), and performing the integral over ω'' by closing the contour in the upper half of the complex plane, we find

$$\Sigma^{\text{FM}}_{n\mathbf{k},n'\mathbf{k}'}(\omega) = \frac{1}{N_p^2} \sum_{mm'\mathbf{q}\nu} g^*_{mn\nu}(\mathbf{k},\mathbf{q})\, g_{m'n'\nu}(\mathbf{k}',\mathbf{q}) \sum_s A^s_{m\mathbf{k}+\mathbf{q}}\left(A^s_{m'\mathbf{k}'+\mathbf{q}}\right)^* \left[\frac{\theta(\varepsilon_s-\mu)}{\hbar\omega - \varepsilon_s - \hbar\omega_{\mathbf{q}\nu} + i\eta} + \frac{\theta(\mu-\varepsilon_s)}{\hbar\omega - \varepsilon_s + \hbar\omega_{\mathbf{q}\nu} - i\eta} \right],$$ (45)

where θ is the Heaviside function.

C. Self-consistent polaron equations

The self-energies Σ^{P} and Σ^{FM} obtained in the previous section can be used inside the Dyson equation (20) after a transformation to frequency domain:

$$G^{-1}_{n\mathbf{k},n'\mathbf{k}'}(\omega) = (G^0)^{-1}_{n\mathbf{k},n'\mathbf{k}'}(\omega) - \Sigma^{\text{P}}_{n\mathbf{k},n'\mathbf{k}'}(\omega) - \Sigma^{\text{FM}}_{n\mathbf{k},n'\mathbf{k}'}(\omega).$$ (46)

The first term in the right-hand side is obtained from Eq. (16) by using the Fourier representation of the Dirac delta function:

$$(G^0)^{-1}_{n\mathbf{k},n'\mathbf{k}'}(\omega) = (\hbar\omega - \varepsilon_{n\mathbf{k}})\, \delta_{n\mathbf{k},n'\mathbf{k}'}.$$ (47)

Note that $(G^0)^{-1}_{n\mathbf{k},n'\mathbf{k}'}(\omega)$ in Eq. (47), $\Sigma^{\text{P}}_{n\mathbf{k},n'\mathbf{k}'}(\omega)$ in Eq. (41), and $\Sigma^{\text{FM}}_{n\mathbf{k},n'\mathbf{k}'}(\omega)$ in Eq. (45) have dimensions of energy.

We are now in a position to combine the above results into a self-consistent set of equations for the polaron quasiparticle amplitudes. By using Eqs. (34), (39), (41), and (45)–(47), we find that the poles of the interacting Green's function are the solutions of the following eigenvalue problem:

$$\sum_{n'\mathbf{k}'} H^{\text{pol}}_{n\mathbf{k},n'\mathbf{k}'} A^s_{n'\mathbf{k}'} = \varepsilon_s A^s_{n\mathbf{k}},$$ (48)

where the effective polaron Hamiltonian H^{pol} depends on the electron addition and removal energies and quasiparticle amplitudes as follows:

$$H^{\text{pol}}_{n\mathbf{k},n'\mathbf{k}'} = \varepsilon_{n\mathbf{k}}\delta_{n\mathbf{k},n'\mathbf{k}'} - \frac{2}{N_p^2} \sum_{\substack{mm' \\ \nu\mathbf{k}''}} \sum_s^{\varepsilon_s<\mu} A^s_{m'\mathbf{k}''+\mathbf{k}-\mathbf{k}'} \frac{g^*_{m'm\nu}(\mathbf{k}'',\mathbf{k}-\mathbf{k}')}{\hbar\omega_{\mathbf{k}-\mathbf{k}'\nu}} (A^s_{m\mathbf{k}''})^* g_{nn'\nu}(\mathbf{k}',\mathbf{k}-\mathbf{k}')$$

$$+ \frac{1}{N_p^2} \sum_{\substack{mm' \\ \nu\mathbf{q}}} \sum_{s'} g^*_{mn\nu}(\mathbf{k},\mathbf{q})\, g_{mn'\nu}(\mathbf{k}',\mathbf{q}) A^{s'}_{m'\mathbf{k}+\mathbf{q}}(A^{s'}_{m\mathbf{k}'+\mathbf{q}})^* \left[\frac{\theta(\varepsilon_{s'}-\mu)}{\varepsilon_s - \varepsilon_{s'} - \hbar\omega_{\mathbf{q}\nu} + i\eta} + \frac{\theta(\mu-\varepsilon_{s'})}{\varepsilon_s - \varepsilon_{s'} + \hbar\omega_{\mathbf{q}\nu} - i\eta} \right].$$ (49)

The self-consistent solution of Eqs. (48) and (49) yields the excitation energies and the quasiparticle amplitudes of the Dyson orbitals, and hence the polaron energies and wave functions. We note that the only approximations that we have made thus far are the Migdal approximation to the electron-phonon vertex in Eq. (24), and the replacement of the interacting phonon Green's function by its noninteracting (i.e., DFPT) counterpart in Eq. (13).

Equations (48) and (49) constitute the central result of this paper. These equations generalize the polaron equations derived in Refs. [34,35] within the context of DFPT to a many-body Green's function formalism for the polaron quasiparticle amplitudes and excitation energies. Practical strategies for solving these equations are outlined in Sec. IV.

A schematic illustration of the self-consistent procedure required for solving Eqs. (48) and (49) is provided in Fig. 3.
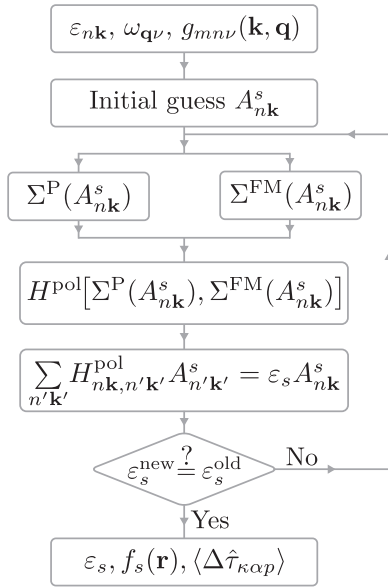
FIG. 3. Schematic representation of the self-consistent procedure required to solve the many-body polaron equations (48) and (49).

D. Total energy of the polaron ground state

In this section, we derive an expression for the total energy of the polaronic ground state in terms of the Dyson orbitals and the eigenvalues of Eq. (48). We proceed along the same lines as for the Galitskii-Migdal formula [79,80], except that we consider the coupled electron-phonon Hamiltonian in Eq. (1).

Upon acting on Eq. (6) with $\hat{c}_{n'\mathbf{k}'}^\dagger(t')$ and taking the expectation value over the ground state, we find

$$
\begin{aligned}
i\hbar &\frac{\partial}{\partial t} \langle \hat{c}_{n'\mathbf{k}'}^\dagger(t')\hat{c}_{n\mathbf{k}}(t)\rangle \\
&= \varepsilon_{n\mathbf{k}}\langle \hat{c}_{n'\mathbf{k}'}^\dagger(t')\hat{c}_{n\mathbf{k}}(t)\rangle + N_p^{-\frac{1}{2}} \\
&\times \sum_{n'\mathbf{q}\nu} g_{nn'\nu}(\mathbf{k}-\mathbf{q},\mathbf{q})\langle \hat{c}_{n'\mathbf{k}'}^\dagger(t')\hat{c}_{n'\mathbf{k}-\mathbf{q}}(t)(\hat{a}_{\mathbf{q}\nu}+\hat{a}_{-\mathbf{q}\nu}^\dagger)\rangle. \quad (50)
\end{aligned}
$$

This expression can be related to the total energy $E = \langle \hat{H}\rangle$ by taking the expectation value of the electron-phonon Hamiltonian in Eq. (1):

$$
\begin{aligned}
E = \lim_{\substack{t'\to t^+ \\ n'\mathbf{k}'=n\mathbf{k}}} \sum_{n\mathbf{k}} i\hbar \frac{\partial}{\partial t}\langle \hat{c}_{n'\mathbf{k}'}^\dagger(t')\hat{c}_{n\mathbf{k}}(t)\rangle \\
+ \sum_{\mathbf{q}\nu} \hbar\omega_{\mathbf{q}\nu}(\langle \hat{a}_{\mathbf{q}\nu}^\dagger \hat{a}_{\mathbf{q}\nu}\rangle + 1/2). \quad (51)
\end{aligned}
$$

The first term on the right-hand side of this expression can be identified with the electron Green's function from Eq. (5):

$$
\begin{aligned}
E = \lim_{\substack{t'\to t^+ \\ n'\mathbf{k}'=n\mathbf{k}}} \sum_{n\mathbf{k}} \hbar^2 \frac{\partial}{\partial t} G_{n\mathbf{k},n'\mathbf{k}'}(t,t') \\
+ \sum_{\mathbf{q}\nu} \hbar\omega_{\mathbf{q}\nu}(\langle \hat{a}_{\mathbf{q}\nu}^\dagger \hat{a}_{\mathbf{q}\nu}\rangle + 1/2). \quad (52)
\end{aligned}
$$

We transform this result into the frequency domain, and we make use of the spectral representation of the Green's function

[80]

$$
\begin{aligned}
E = &-\sum_{n\mathbf{k}} \frac{\hbar^2}{\pi} \int_{-\infty}^{\mu} d\omega\, \omega\, \mathrm{Im}[G_{n\mathbf{k},n\mathbf{k}}(\omega)] \\
&+ \sum_{\mathbf{q}\nu} \hbar\omega_{\mathbf{q}\nu}(\langle \hat{a}_{\mathbf{q}\nu}^\dagger \hat{a}_{\mathbf{q}\nu}\rangle + 1/2). \quad (53)
\end{aligned}
$$

By further using the Lehmann representation in Eq. (34) and the expansion of the Dyson orbitals in terms of polaron quasiparticle amplitudes, Eq. (39), we obtain

$$
E = \frac{1}{N_p} \sum_{n\mathbf{k}} \sum_{s}^{\varepsilon_s<\mu} \varepsilon_s |A_{n\mathbf{k}}^s|^2 + \sum_{\mathbf{q}\nu} \hbar\omega_{\mathbf{q}\nu}(\langle \hat{a}_{\mathbf{q}\nu}^\dagger \hat{a}_{\mathbf{q}\nu}\rangle + 1/2). \quad (54)
$$

In the second term on the right-hand side, the expectation value of the phonon number operator must also be related to the polaron quasiparticle amplitudes $A_{n\mathbf{k}}^s$. We have not found a way to establish this relation in the most general case. However, an accurate first-principles formulation is still possible if we make the approximation that the phonon subsystem can be described as a superposition of coherent states.

Coherent states are minimum-uncertainty wave packets, and in the case of the harmonic oscillator they correspond to Gaussian wave functions, rigidly translated away from the minimum of the potential well. The reason for considering coherent states is that much of the earlier literature on the Fröhlich polaron model shows how coherent states constitute a very accurate variational ansatz for determining the ground-state energy of the polaron [81–86].

We therefore approximate the phonon subsystem of the polaron ground state as the following normalized superposition of coherent states:

$$
|N+1\rangle = \exp\left[\sum_{\mathbf{q}\nu}\left(u_{\mathbf{q}\nu}\hat{a}_{\mathbf{q}\nu}^\dagger - |u_{\mathbf{q}\nu}|^2/2\right)\right]|N+1, 0_{\mathrm{ph}}\rangle, \quad (55)
$$

where $u_{\mathbf{q}\nu}$ indicates the (complex) displacement of the wave packet and $|0_{\mathrm{ph}}\rangle$ denotes the phonon vacuum. With this approximation, we have the standard property $\hat{a}_{\mathbf{q}\nu}|N+1\rangle = u_{\mathbf{q}\nu}|N+1\rangle$. By using this relation inside Eqs. (54), (2), and (40), and employing time-reversal symmetry to replace $u_{-\mathbf{q}\nu}^*$ by $u_{\mathbf{q}\nu}$, we can rewrite the total energy as

$$
E = \frac{1}{N_p} \sum_{n\mathbf{k}} \sum_{s}^{\varepsilon_s<\mu} \varepsilon_s |A_{n\mathbf{k}}^s|^2 + \sum_{\mathbf{q}\nu} \hbar\omega_{\mathbf{q}\nu}(|u_{\mathbf{q}\nu}|^2 + 1/2), \quad (56)
$$

where the coherent displacements are given by

$$
u_{\mathbf{q}\nu} = -N_p^{-3/2} \sum_{s}^{\varepsilon_s<\mu} \sum_{\mathbf{k}nn'} A_{n'\mathbf{k}+\mathbf{q}}^s \frac{g_{n'n\nu}^*(\mathbf{k},\mathbf{q})}{\hbar\omega_{\mathbf{q}\nu}}(A_{n\mathbf{k}}^s)^*. \quad (57)
$$

The last two equations provide the relation between the total ground-state energy of an interacting electron-phonon system, and the excitation energies and quasiparticle amplitudes of the Dyson orbitals, within the approximation of coherent states for the phonon subsystem. From the second term on the right-hand side of Eq. (56), we see that $|u_{\mathbf{q}\nu}|^2$ gives the number of phonons $\mathbf{q}\nu$ (per BvK supercell) contributing to the polaronic lattice distortion.

IV. TOWARD *AB INITIO* CALCULATIONS

A. Approximations for practical calculations

The formalism developed in Sec. III provides a self-consistent mathematical framework to investigate polaron wave functions and formation energies within a first-principles many-body approach. However, the self-consistent solution of Eqs. (48) and (49) is currently beyond reach for real materials because it requires a summation over all the occupied and unoccupied polaronic states in the Fan-Migdal self-energy term, including those with finite total polaron momentum.

In view of devising a practical approach for systematic many-body *ab initio* calculations of polarons, we make the following reasoning. If we approximate the interacting many-body ground state by a single Slater determinant, and assume that the added electron in the $(N + 1)$-electron system has a negligible effect on the lowest-N electron wave functions and energies, the contributions of the valence states in the N- and $(N + 1)$-electron systems in Eq. (54) are identical. This approximation is physically motivated by the fact that the addition of a single electron to a system of many electrons will modify the electron density only slightly [35]. Furthermore, by construction, the N-electron system is associated with a periodic undistorted lattice, therefore, the expectation value of the phonon number operator vanishes in $\langle N|\hat{H}|N\rangle$. These observations lead to the following simplified expression for the formation energy of the polaron in the BvK supercell[1]:

$$
\Delta E = \langle N + 1|\hat{H}|N + 1\rangle - \left(\langle N|\hat{H}|N\rangle + \varepsilon_{\text{CBM}}^{\text{QP}}\right)
$$
$$
= \varepsilon_{s,\text{min}} - \varepsilon_{\text{CBM}}^{\text{QP}} + \sum_{\mathbf{q}\nu} \hbar\omega_{\mathbf{q}\nu}|u_{\mathbf{q}\nu}|^2. \quad (58)
$$

In this expression, $\varepsilon_{\text{CBM}}^{\text{QP}}$ represents the many-body electron addition energy for the periodic, undistorted lattice. For example, this could be the quasiparticle energy of the conduction band bottom in a GW calculation in the absence of atomic displacements. A schematic illustration of Eq. (58) is given in Fig. 2. The quantity E_{lattice} appearing in the figure corresponds to the last term of Eq. (58), where the coherent displacements are given by Eq. (57).

Similarly, we obtain a compact expression for the polaronic self-energy Σ^{P} by replacing the first N occupied states with unperturbed Bloch wave functions With this choice, the quasiparticle amplitudes for these states become Dirac delta functions, $A_{n\mathbf{k}}^s = \sqrt{N_p}\,\delta_{s,n\mathbf{k}}$, and their contribution to Σ^{P} can be neglected in Eq. (41). As a result, only the lowest-energy Dyson orbital, which corresponds to the electronic part of the polaron wave function (cf. Sec. III A), contributes in the summation in Eq. (41):

$$
\Sigma_{n\mathbf{k},n'\mathbf{k}'}^{\text{P}} = -\frac{2}{N_p^2} \sum_{mm'\nu\mathbf{k}''} g_{nn'\nu}(\mathbf{k}', \mathbf{k} - \mathbf{k}')
$$
$$
\times A_{m'\mathbf{k}''+\mathbf{k}-\mathbf{k}'}^{s,\text{min}} \frac{g_{m'm\nu}^*(\mathbf{k}'', \mathbf{k} - \mathbf{k}')}{\hbar\omega_{\mathbf{k}-\mathbf{k}'\nu}}(A_{m\mathbf{k}''}^{s,\text{min}})^*. \quad (59)
$$

---

[1]The equivalent expression for the formation energy of a hole polaron upon electron removal is $\Delta E = -(\varepsilon_{s,\text{min}} - \varepsilon_{\text{VBM}}^{\text{QP}}) + \sum_{\mathbf{q}\nu} \hbar\omega_{\mathbf{q}\nu}|u_{\mathbf{q}\nu}|^2$.

A similar reasoning can be extended to the self-energy Σ^{FM} in Eq. (42). We replace the interacting Green's function G by its noninteracting counterpart G^0. This choice amounts to assuming sharp quasiparticles, as in the standard G_0W_0 approximation [48]. With this replacement, Σ^{FM} becomes diagonal in the single-particle basis, and simplifies to

$$
\Sigma_{n\mathbf{k},n'\mathbf{k}'}^{\text{FM}}(\omega) = \frac{\delta_{n\mathbf{k},n'\mathbf{k}'}}{N_p} \sum_{m\mathbf{q}\nu} |g_{mn\nu}(\mathbf{k}, \mathbf{q})|^2
$$
$$
\times \left[\frac{\theta(\varepsilon_{m\mathbf{k}+\mathbf{q}} - \mu)}{\hbar\omega - \varepsilon_{m\mathbf{k}+\mathbf{q}} - \hbar\omega_{\mathbf{q}\nu} + i\eta} \right.
$$
$$
\left. + \frac{\theta(\mu - \varepsilon_{m\mathbf{k}+\mathbf{q}})}{\hbar\omega - \varepsilon_{m\mathbf{k}+\mathbf{q}} + \hbar\omega_{\mathbf{q}\nu} - i\eta} \right]. \quad (60)
$$

This expression only depends on the phonon frequencies and the electron-phonon matrix elements of the periodic configuration. Equation (60) is the standard expression used in *ab initio* calculations of electron-phonon renormalization of band structures [33].

Using the above simplifications, the many-body polaron equations are reduced to solving the self-consistent eigenvalue problem given by

$$
\sum_{n'\mathbf{k}'} \left\{ \varepsilon_{n\mathbf{k}}\delta_{n\mathbf{k},n'\mathbf{k}'} + \Sigma_{n\mathbf{k},n'\mathbf{k}'}^{\text{P}} + \Sigma_{n\mathbf{k},n'\mathbf{k}'}^{\text{FM}}(\varepsilon_{s,\text{min}}/\hbar) \right\} A_{n'\mathbf{k}'}^{s,\text{min}}
$$
$$
= \varepsilon_{s,\text{min}} A_{n\mathbf{k}}^{s,\text{min}}, \quad (61)
$$

where the self-energies are given by Eqs. (59) and (60). In the remainder of this paper, the index s_{min} corresponding to the wave function and eigenvalue of the polaron in the ground state will be omitted for ease of notation.

B. Relation to the theory of Ref. [35]

The many-body polaron equations (59)–(61) share a similar form with the DFPT polaron equations derived in Ref. [35] [see Eqs. (37) and (38) of that work]. In fact, if we neglect the Fan-Migdal self-energy term in Eq. (61), the two sets of equations become identical within the approximations outlined in Sec. IV A.

The main differences between the two approaches are that, in the present case, (i) the polaron eigenvalue also incorporates the dynamical Fan-Migdal self-energy renormalization, and (ii) the lattice distortion energy in Eq. (54) is directly linked to the number of phonons that participate in the polaron via the phonon number operator $\hat{a}_{\mathbf{q}\nu}^\dagger \hat{a}_{\mathbf{q}\nu}$.

The fact that we reached a very similar set of polaron equations as in Ref. [35] starting from a general many-body formulation is very encouraging, and provides a rigorous field-theoretic justification for the DFPT approach followed in Ref. [35].

At a qualitative level, the main improvement of the present many-body approach over the DFPT strategy of Ref. [35] is in that our present formalism incorporates dynamical effects as described by the FM self-energy. Therefore, in addition to the physics of phonon-induced localization and self-trapping, the present approach also captures the physics of phonon-induced band-structure renormalization and polaron satellites in photoemission spectra.

C. Perturbation theory on the polaron quasiparticle amplitudes and energies

Equations (59)–(61) constitute a nonlinear, self-consistent eigenvalue problem. The polaron energy ε appears on both sides of Eq. (61), therefore, an iterative solution is required.

This requirement can be relaxed if we proceed to evaluate the equations in perturbation theory. Specifically, one could solve the equations by retaining only Σ^{P} and treating Σ^{FM} within perturbation theory, or vice versa by retaining Σ^{FM} and treating Σ^{P} perturbatively. Since Σ^{FM} does not couple different wave vectors, the latter option would lead to a vanishing polaronic correction and no localization, which is equivalent to standard calculations of band renormalization in absence of polarons. Therefore, we focus on the former option of retaining only the polaronic self-energy and treating the FM term perturbatively. This procedure can be implemented in two steps:

(i) Solve Eq. (61) by considering only the polaronic self-energy Σ^{P}:

$$\sum_{n'\mathbf{k}'} \left\{ \varepsilon_{n\mathbf{k}} \delta_{n\mathbf{k},n'\mathbf{k}'} + \Sigma^{\mathrm{P}}_{n\mathbf{k},n'\mathbf{k}'} \right\} A^{\mathrm{P}}_{n'\mathbf{k}'} = \varepsilon^{\mathrm{P}} A^{\mathrm{P}}_{n\mathbf{k}}. \tag{62}$$

(ii) Add the FM contribution to the polaron energy after replacing $A_{n\mathbf{k}}$ by the solution at the previous step $A^{\mathrm{P}}_{n\mathbf{k}}$:

$$\varepsilon = \frac{1}{N_p} \sum_{n\mathbf{k}} \sum_{n'\mathbf{k}'} A^{\mathrm{P},*}_{n\mathbf{k}} \left(\varepsilon_{n\mathbf{k}} \delta_{n\mathbf{k},n'\mathbf{k}'} + \Sigma^{\mathrm{P}}_{n\mathbf{k},n'\mathbf{k}'} \right) A^{\mathrm{P}}_{n'\mathbf{k}'}$$
$$+ \frac{1}{N_p} \sum_{n\mathbf{k}} \left| A^{\mathrm{P}}_{n\mathbf{k}} \right|^2 \Sigma^{\mathrm{FM}}_{n\mathbf{k}}(\omega). \tag{63}$$

Within the simplest Rayleigh-Schrödinger perturbation theory, the frequency ω appearing in the last equation can either be set the polaron eigenvalue $\omega = \varepsilon^{\mathrm{P}}/\hbar$ or to the unperturbed Bloch eigenvalue $\omega = \varepsilon^0/\hbar$. In Sec. V A we compare the latter to the self-consistent solution of Eq. (61).

V. APPLICATIONS

A. Fröhlich model

To validate the theory developed in Secs. II–IV, we apply the formalism to the Fröhlich model [5,6,20]. The Fröhlich model represents a standard benchmark in the study of polaron physics, and has been investigated by a number of authors using a variety of many-body techniques [4,21,26,28,29,32,87]. The availability of highly accurate solutions such as Feynman's path-integral results [26] and diagrammatic Monte Carlo calculations [29] makes it possible to carefully assess the validity of our approach and of the approximations described in Sec. IV.

In the Fröhlich model, the Hamiltonian given by Eq. (1) is simplified by considering a single-electron band with effective mass m^* and parabolic dispersions $\varepsilon_{\mathbf{k}} = \hbar^2 |\mathbf{k}|^2 / 2m^*$, coupled to a dispersionless longitudinal polar optical phonon with frequency ω_{LO}. The coupling matrix element is given by [21,88]

$$g(\mathbf{q}) = \frac{i}{|\mathbf{q}|} \left[\frac{e^2}{4\pi\epsilon_0} \frac{4\pi}{\Omega} \frac{\hbar\omega_{\mathrm{LO}}}{2} \frac{1}{\kappa} \right]^{1/2}. \tag{64}$$

In this equation, ϵ_0 is the vacuum permittivity, and the dielectric screening constant κ is defined by $1/\kappa = 1/\epsilon^\infty - 1/\epsilon^0$, with ϵ^∞ and ϵ^0 being the high-frequency electronic permittivity and the static dielectric constant including the ionic contribution, respectively. In this model, the Debye-Waller self-energy vanishes [89], and the electron-phonon coupling strength is traditionally described by a single parameter α, referred to as the Fröhlich coupling constant [25,35,90]

$$\alpha = \frac{e^2}{4\pi\epsilon_0} \frac{1}{\hbar} \sqrt{\frac{m^*}{2\hbar\omega_{\mathrm{LO}}}} \frac{1}{\kappa}. \tag{65}$$

There is a single Dyson orbital, which we identify with the electronic part of the polaron wave function, $f(\mathbf{r}) = \psi(\mathbf{r})$. The expansion in Eq. (39) can now be performed in terms of plane waves, and the transition to the extended crystal is performed by considering an infinite number of unit cells in the BvK supercell so that summations over the momentum $\mathbf{k}$ become continuous integrals:

$$\psi(\mathbf{r}) = \frac{\sqrt{\Omega}}{(2\pi)^3} \int d\mathbf{k} \, A(\mathbf{k}) \, e^{i\mathbf{k}\cdot\mathbf{r}}. \tag{66}$$

Here, $\mathbf{r}$ and $\mathbf{k}$ belong to $\mathbb{R}^3$, and Ω is the unit-cell volume. We require that the polaron wave function be normalized in real space,

$$\int d\mathbf{r} \, |\psi(\mathbf{r})|^2 = 1, \tag{67}$$

and this implies the normalization of its Fourier coefficients:

$$\frac{\Omega}{(2\pi)^3} \int d\mathbf{k} \, |A(\mathbf{k})|^2 = 1. \tag{68}$$

Using Eqs. (66) and (68) inside Eq. (61), we obtain

$$\varepsilon = \frac{\Omega}{(2\pi)^3} \int d\mathbf{k} A(\mathbf{k}) \int d\mathbf{k}' \left[\varepsilon_{\mathbf{k}} \, \delta(\mathbf{k} - \mathbf{k}') \right.$$
$$\left. + \Sigma^{\mathrm{P}}(\mathbf{k}, \mathbf{k}') + \Sigma^{\mathrm{FM}}(\mathbf{k}; \varepsilon) \, \delta(\mathbf{k} - \mathbf{k}') \right] A(\mathbf{k}'). \tag{69}$$

Using Eq. (59), the polaronic self-energy appearing in this expression becomes

$$\Sigma^{\mathrm{P}}(\mathbf{k}, \mathbf{k}') = -\frac{2\Omega^2}{(2\pi)^6} \frac{|g(\mathbf{k} - \mathbf{k}')|^2}{\hbar\omega_{\mathrm{LO}}} \int d\mathbf{k}'' A_{\mathbf{k}''+\mathbf{k}-\mathbf{k}'} A^*_{\mathbf{k}''}. \tag{70}$$

The FM self-energy in Eq. (60) can be evaluated exactly [90] and is given by

$$\Sigma^{\mathrm{FM}}(\mathbf{k}; \varepsilon) = -\frac{\alpha \, (\hbar\omega_{\mathrm{LO}})^{3/2}}{\sqrt{\varepsilon_{\mathbf{k}}}} \arcsin\left(\sqrt{\frac{\varepsilon_{\mathbf{k}}}{\hbar\omega_{\mathrm{LO}} - \varepsilon + \varepsilon_{\mathbf{k}}}} \right). \tag{71}$$

To calculate the energy and wave function of the lowest polaron state, we use a variational approach. For simplicity, following Refs. [25,35], for the electronic part we employ a normalized exponential trial wave function:

$$\psi(\mathbf{r}; r_p) = \sqrt{\frac{1}{\pi r_p^3}} \exp\left[-|\mathbf{r}|/r_p \right], \tag{72}$$

(a)

$\psi(\mathbf{r}; r_p)$ (arb.u.)

(b)

$A(\mathbf{k}; r_p)$ (arb.u.)
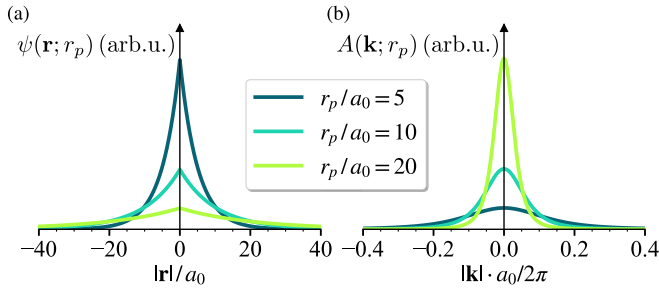
$r_p/a_0 = 5$
$r_p/a_0 = 10$
$r_p/a_0 = 20$

FIG. 4. Variational ansatz for the electronic component of the polaron wave function in the Fröhlich model. (a) Wave-function plot for a few values of the variational parameter r_p, which corresponds to the polaron radius, from Eq. (72). a_0 is the Bohr radius. (b) Reciprocal-space coefficients of the wave functions shown in (a), from Eq. (73).

where r_p can be identified as the polaron radius. The Fourier transform of this function is

$$A(\mathbf{k}; r_p) = 8\sqrt{\frac{\pi r_p^3}{\Omega}} \frac{1}{(r_p^2 |\mathbf{k}|^2 + 1)^2}. \tag{73}$$

Equations (72) and (73) show that the more localized the wave function is in real space (small r_p), the more extended are its coefficients in Fourier space, and vice versa. In Fig. 4, we show the exponential trial wave function for different values of the polaron radius r_p, together with the corresponding Fourier transforms.

We now use Eq. (73) in Eq. (69), and evaluate the integrals for each of the three terms within square brackets. The first term is the average of the kinetic energy:

$$\frac{\Omega}{(2\pi)^3} \int d\mathbf{k}\, A^*(\mathbf{k}; r_p) \frac{\hbar |\mathbf{k}|^2}{2m^*} A(\mathbf{k}; r_p) = \frac{\hbar}{2m^* r_p^2}, \tag{74}$$

and is identical to what is found in the Landau-Pekar model [25,35]. The expectation value of the term containing Σ^P in Eq. (69) corresponds to the Coulomb energy in the Landau-Pekar model, and is given by [25,35]

$$\langle \Sigma^P \rangle = -\frac{e^2}{4\pi\epsilon_0} \frac{1}{\kappa} \frac{5}{8} \frac{1}{r_p}. \tag{75}$$

From Eqs. (69) and (73), we see that the expectation value of the FM self-energy results from the radial integral:

$$\langle \Sigma^{FM} \rangle = \frac{\Omega}{(2\pi)^3} 4\pi \int_0^\infty dk\, |A(k; r_p)|^2\, \Sigma^{FM}(k). \tag{76}$$

Let us analyze the asymptotic limits of this integral. In the limit of a strongly localized polaron ($r_p \to 0$), $A(k)$ tends to a constant value, but $\Sigma^{FM}(k)$ is significant only near $k = 0$ [cf. Eq. (71)]. Owing to the normalization of the Fourier coefficients, the integral vanishes in this limit. In the limit of an extended polaron ($r_p \to \infty$), the $A(k)$ coefficients become a Dirac delta function centered at $k = 0$, therefore, the integral coincides with the value of the FM self-energy at $k = 0$, $\langle \Sigma^{FM} \rangle = -\alpha \hbar \omega_{LO}$ (having set $\varepsilon = 0$).

Equations (74)–(76) allow us to evaluate the polaron eigenvalue as a function of the polaron radius $\varepsilon(r_p)$. To determine the total formation energy, we also need to consider the lattice

relaxation energy, i.e., the last term in Eq. (58). The evaluation of this term yields

$$\int d\mathbf{q}\, \hbar\omega_{\mathbf{q}} \langle \hat{a}_{\mathbf{q}}^\dagger \hat{a}_{\mathbf{q}} \rangle = \frac{\Omega^3}{(2\pi)^9} \int d\mathbf{q}\, \frac{|g(\mathbf{q})|^2}{\hbar\omega_{LO}}$$
$$\times \int d\mathbf{k} \int d\mathbf{k}'\, (A_{\mathbf{k}+\mathbf{q}})^* A_{\mathbf{k}} A_{\mathbf{k}'+\mathbf{q}} (A_{\mathbf{k}'})^*$$
$$= \frac{e^2}{4\pi\epsilon_0} \frac{1}{\kappa} \frac{5}{16} \frac{1}{r_p}. \tag{77}$$

Putting together the above results, we obtain the following expression for the total energy of the Fröhlich polaron as a function of the radius r_p:

$$\Delta E(r_p) = \frac{\hbar}{2m^* r_p^2} - \frac{5}{16} \frac{e^2}{4\pi\epsilon_0\kappa} \frac{1}{r_p}$$
$$+ \frac{2^8 \pi^2 r_p^3}{\Omega} \int_0^\infty dk\, \frac{\Sigma^{FM}(k)}{(1 + r_p^2 k^2)^4}, \tag{78}$$

where Σ^{FM} is given by Eq. (71). This total energy coincides with the energy of the Landau-Pekar model if we neglect the integral on the right-hand side [see, for example, Eq. (10) of Ref. [35]]. We note that the polaron formation energy within the Fröhlich model has been called E in previous work because the delocalized state with no electron-phonon interaction has zero total energy by definition.

In Fig. 5 we analyze the total energy as a function of the polaron radius r_p. In this example, the physical parameters have been chosen to match those for the electron polaron in LiF [35], namely, $m^* = 0.88\, m_e$, $\hbar\omega_{LO} = 77$ meV, $\epsilon^0 = 10.62$, and $\epsilon^\infty = 2.04$, giving a coupling constant of $\alpha = 4.94$. Figure 5(a) illustrates the contribution to the polaron energy from each term in Eq. (78). The first term on the right-hand side of Eq. (78) is the kinetic energy (dotted line). This term is positive and thus favors delocalization. The second term on the right-hand side of Eq. (78) is the Coulomb attraction energy between the electron and the lattice distortion (dashed-dotted line). This term is negative and thus favors localization. The last term in Eq. (78) is the FM self-energy contribution. It is negative and thus it also favors localization, but it varies more smoothly with the radius. As discussed above, this term tends to vanish at small radius, and approaches the value $-\alpha \hbar \omega_{LO}$ at large radius.

Figure 5(b) shows the dependence of the total energy of the polaron on the radius (blue line). The minimum of this energy is marked by a cross and indicates the variational solution. For the sake of comparison, we also show the total-energy curve for the Landau-Pekar model (red line) [35]. In this model there is no FM contribution. We see that the FM contribution modifies the shape of the energy surface of the Landau-Pekar model, and shifts the minimum towards a larger radius and a lower ground-state energy.

Now we analyze the dependence of the variational polaron energy on the coupling constant α. To this aim, we generate curves like those in Fig. 5(b) for a range of parameters α, and we determine the minimum in each case. The results are reported in Fig. 6.

In Fig. 6(a), the red line represents the Landau-Pekar ground-state polaron formation energy. Within the exponen-
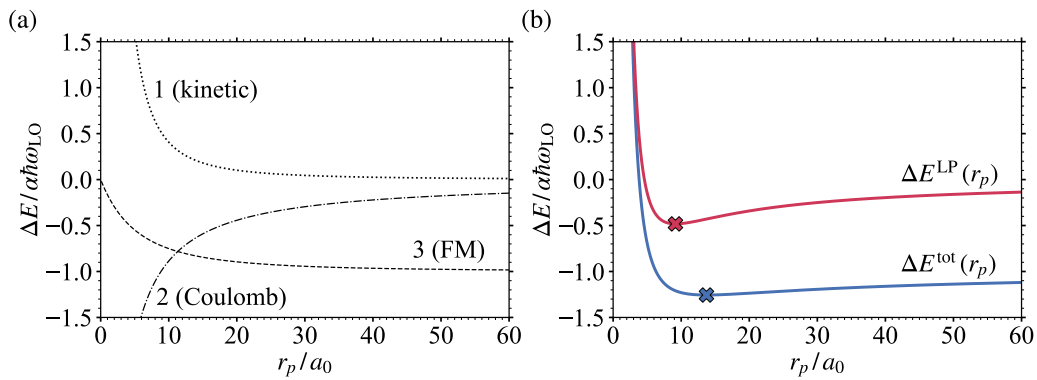
FIG. 5. Ground-state polaron energy as a function of the polaron radius r_p, within the Fröhlich model for $\alpha = 4.94$. (a) r_p dependence of the different terms contributing to the total energy in Eq. (78), namely, the kinetic energy (dotted), the Coulomb energy composed by the Landau-Pekar and the lattice energy (dotted-dashed), and the Fan-Migdal self-energy contribution (dashed). (b) Total energy as a function of the polaron radius r_p. The red solid line represents the Landau-Pekar result [35], where only the kinetic and the Coulomb energies are considered. The blue solid line represents the total energy including the FM contribution, as in Eq. (78). The energy minima are highlighted by the solid crosses.

tial ansatz used in Eq. (72), this energy is given by $\Delta E^{LP} = -(50/512)\alpha^2\hbar\omega_{LO}$ [35]. The blue line represents the FM self-energy evaluated within Rayleigh-Schrödinger perturbation theory, and is given by $\Delta E^{FM,RS} = -\alpha\hbar\omega_{LO}$ [90]. The gray line represents the result obtained by Feynman's path-integral method [26,91,92], and the black circles are diagrammatic Monte Carlo results [28,29,93]. This comparison shows that Feynman's results are essentially as accurate as the diagrammatic Monte Carlo data, therefore, in the following we use Feynman's result as the "exact" solution for the purpose of comparison.

In Fig. 6(b) we show the relative errors of the Landau-Pekar (LP) energy and the Fan-Migdal energy (in the Rayleigh-Schrödinger approximation, FM-RS) with respect

to Feynman's result as filled areas, following the same color convention as in Fig. 6(a). It is clear that both approaches deviate significantly from Feynman's result throughout the entire coupling range, with errors in the energy as large as 100%. The LP result gives the correct trend at strong couplings, but it underestimates the polaron energy at weak couplings. In contrast, the FM-RS result correctly captures the linear dependence of the energy at weak couplings, but it underestimates the polaron energy at strong couplings.

In Figs. 6(c) and 6(d) we compare the total energy of the polaron calculated using Eq. (78) with the Feynman theory. We compare two different levels of approximation. First, we compute the polaron ground-state energy by requiring self-consistency in the energy entering the FM self-energy, as in
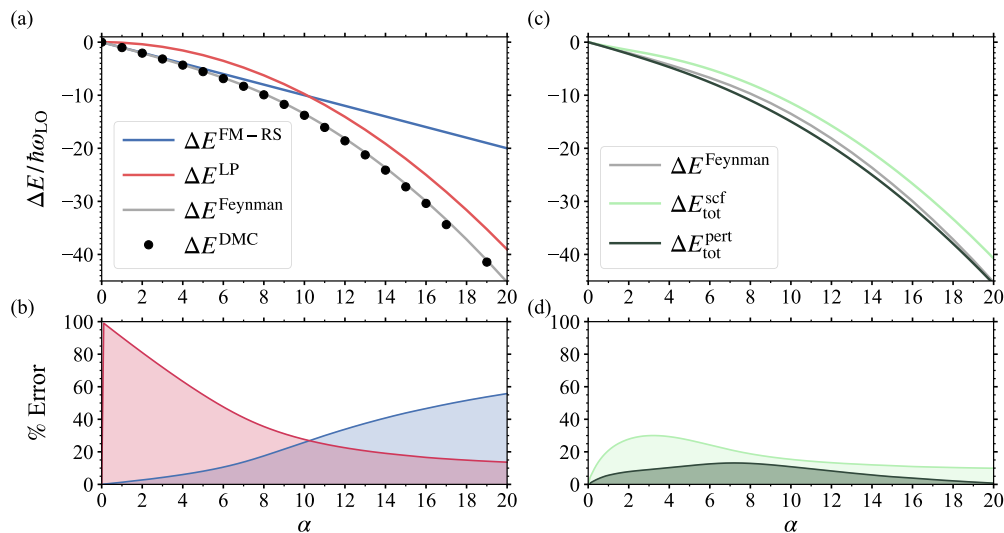

FIG. 6. Total energy of the ground state of the Fröhlich polaron as a function of the coupling strength α. (a) Fan-Migdal solution in Rayleigh-Schrödinger perturbation theory (FM-RS, blue line), Landau-Pekar solution (LP, red line), Feynman's variational path-integral solution (gray line) [26,91,92], and diagrammatic Monte Carlo results (DMC, black circles) [28,29,93]. (b) Relative deviation between FM-RS and LP energies with respect to Feynman's result, following the same color scheme as in (a). (c) Ground-state energy of the Fröhlich polaron evaluated using the present Green's function approach. The light green line represents the self-consistent solution, the dark-green line represents the perturbative calculation. The relative errors of each approximation with respect to Feynman's result are shown in (d).

Eq. (61). We will denote the ground-state energy obtained in this way by $\Delta E_{\text{tot}}^{\text{scf}}$. Second, we consider the perturbative approach discussed in Sec. IV C. Within the Fröhlich model, this translates to the following two-step process for each coupling constant α:

(i) We determine the polaron radius that minimizes the Landau-Pekar total energy. With the exponential ansatz of Eq. (72), this radius is $r_{p,\text{min}} = 16\kappa m_e a_0/5m^*$ [35].

(ii) We calculate the total formation energy of the polaron by adding the FM contribution evaluated at the noninteracting energy as a perturbation:

$$\Delta E_{\text{tot}}^{\text{pert}} = -\frac{50}{512}\alpha^2 \hbar\omega_{\text{LO}}$$
$$+ 4\pi \int_0^\infty dk\, |A(k; r_{p,\text{min}})|^2\, \Sigma^{\text{FM}}(k; \varepsilon = 0). \quad (79)$$

The result of these two approaches is shown in Fig. 6(c) as light green and dark green lines, respectively. The results by Feynman are shown as the dashed gray line. The filled areas in Fig. 6(d) represent the relative errors with respect to Feynman's result, with the same color code as in Fig. 6(c). This comparison indicates that our formalism correctly describes the polaron energy throughout the entire range of couplings, irrespective of the level of approximation adopted in the evaluation of the ground-state energy. Interestingly, the deviation of the perturbative approach with respect to Feynman's results never exceeds 10%. This success suggests that the perturbative procedure is particularly suitable for studying polarons, and can be generalized to *ab initio* calculations.

The variational ansatz employed in Eq. (72) could be improved further [6,25,94], therefore, we expect that with some refinements we should be able to achieve an even better agreement with Feynman's theory. Since no other theoretical approach has succeeded to match Feynman's calculations at all couplings [4], the present results are very encouraging, especially because the present approach can be used for *ab initio* calculations of real materials, as we show in Sec. V B.

B. *Ab initio* calculations in LiF

As a first fully *ab initio* calculation using the methodology presented in this work, we compute the polaronic band-gap renormalization of LiF from first principles. To this aim, we consider the simplest approximation to our theory, as described in Sec. IV C. In this section we provide the details of the computational procedure, while the main results and implications are discussed in the companion paper [47].

All calculations are performed using the QUANTUM ESPRESSO software suite [95]. Ground-state DFT calculations are performed within the Perdew-Burke-Ernzerhof generalized gradient approximation [96], using optimized norm-conserving Vanderbilt (ONCV) pseudopotentials [97,98] and plane waves with a kinetic energy cutoff of 100 Ry. Our optimized lattice parameter is $a = 4.06$ Å. Phonon frequencies and electron-phonon matrix elements are computed within density functional perturbation theory [49]. Coarse momentum grids of $12 \times 12 \times 12$ **k** and **q** points are used for the ground-state electron and lattice dynamics calculations, respectively. Electron energies, phonon frequencies, and electron-phonon matrix elements are interpolated to dense momentum

grids by means of Wannier-Fourier interpolation [99–101], as implemented in the WANNIER90 [102] and EPW [103] codes. The method presented in Ref. [88] is used to deal with the long-range part of the electron-phonon matrix element for polar materials.

In order to converge both the band and momentum sums needed to compute the FM self-energy in Eq. (60) we proceed as follows. Following Refs. [64,104], we divide the band sum into two subspaces: (i) a lower subspace formed by the valence band manifold and the first four conduction bands ($\sim$15 eV above the conduction band bottom), where the momentum integration is carried out explicitly, and (ii) an upper subspace formed by the rest of the conduction bands, where the phonon frequency in the denominator of Eq. (60) is neglected and the band summation is transformed into the solution of a Sternheimer equation [64]. For the solution of the Sternheimer equation and the calculation of the upper subspace contribution, we employ the implementation of Ref. [104] within the PHONON code. The lower subspace contribution is calculated with EPW. A slightly modified version of the code is used to evaluate the FM self-energy at the noninteracting polaron energy for all **k** points, which corresponds to the Kohn-Sham energies of the band extrema. The momentum integrals are converged by interpolating all quantities into fine $96 \times 96 \times 96$ **q**-point grids for each $\Sigma_{\mathbf{k}}^{\text{FM}}$.

Equations (59) and (62) are solved iteratively using the implementation of Refs. [34,35] within EPW. We initialize the $A_{n\mathbf{k}}$ coefficients using a Gaussian line shape centered at the band edge. We note that, similar to a DFT optimization, different initializations could potentially lead to multiple local minima. We validate the robustness of our results by starting the iterative procedure with different Gaussian widths, as well as with random distributions of the $A_{n\mathbf{k}}$ coefficients, for which equivalent self-consistent solutions are obtained within the convergence threshold in all cases. The lattice energy is evaluated using Eqs. (57) and (58). We use increasingly denser **k**-point grids, and we take the isolated polaron limit by extrapolating to infinite supercell size (infinitely dense **k**-point grid) [35].

To assess the validity of the approximation that the change in the total density is negligible upon electron addition and removal (see Sec. IV A) in the worst-case scenario, we perform direct DFT calculations on a $3 \times 3 \times 3$ supercell of LiF with an electron removed (hole polaron). To mitigate the self-interaction error, we use the Heyd-Scuseria-Ernzerhof (HSE) [105] hybrid functional with an exact exchange fraction parameter of $\alpha_{\text{EXX}} = 0.37$. The atomic positions are relaxed so that forces on each ion are below 10^{-5} Ry/bohr. Figure 7(a) shows the relaxed atomic configuration, together with the wave function of the first unoccupied Kohn-Sham state. The total energy of the relaxed configuration is lower than the total energy obtained for the original periodic configuration with the hole, confirming that the polaronic configuration is more stable. For comparison, in Fig. 7(b) we show the hole polaron wave function and atomic displacements obtained by the solution of Eqs. (59) and (62), which is practically identical to the result shown in Fig. 7(a). This result validates *a posteriori* our initial assumption.

Figures 8(a) and 8(b) show our results for the electron and hole polaron energies in LiF, respectively. The light blue

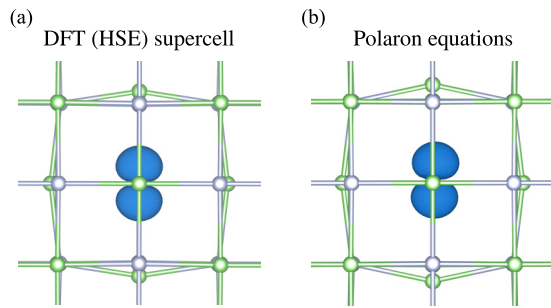(a) DFT (HSE) supercell   (b) Polaron equations

FIG. 7. Comparison between the hole polaron wave function in LiF obtained by (a) direct DFT (HSE) supercell calculation with a removed electron and (b) the solution of the polaron equations in Eqs. (59) and (62).

triangles represent the polaron eigenvalues ε^P as a function of the inverse supercell size, and dark blue crosses represent the corresponding lattice energy in each case. The dashed lines are used to extrapolate these quantities to infinite supercell size. We obtain $\varepsilon^P - \varepsilon_{CBM}^{KS} = -0.898$ eV and $E_{\text{lattice}} = 0.652$ eV for the electron polaron, and $\varepsilon^P - \varepsilon_{VBM}^{KS} = 4.672$ eV and $E_{\text{lattice}} = 2.775$ eV for the hole polaron, in good agreement with the results reported in Ref. [35].

To obtain the total polaron eigenvalue ε from Eq. (63) we need to evaluate the average of the FM self-energy over the quasiparticle amplitudes $A_{n\mathbf{k}}$ obtained above. We accomplish this by performing a Wannier interpolation of the FM self-energy, similar to the Wannier interpolation of the *GW* self-energy corrections to the band structure [106]. This procedure consists of five steps: (i) we calculate the FM self-energy in Eq. (60) on a coarse $8 \times 8 \times 8$ $\mathbf{k}$-point grid; (ii) we add the self-energy to the bare Kohn-Sham eigenvalues on the coarse mesh; (iii) we perform a Wannier interpolation of the bare and the corrected eigenvalues to a fine mesh; (iv) we obtain the interpolated self-energy on the fine mesh from the difference between the bare and the corrected eigenvalues; (v) we evaluate the summation corresponding to the second term on the right-hand side of Eq. (63). Following this procedure, the total computational cost of calculating the full polaronic renormalization of band gaps is approximately given by (i) the cost of performing an adiabatic electron and hole polaron calculation as in Ref. [35], plus (ii) the cost of performing a standard Allen-Heine (AH) based band-structure renormalization calculation on a relatively coarse $\mathbf{k}$-point mesh on the Brillouin zone.

We note that since our Hamiltonian in Eq. (1) only considers electron-phonon interactions to linear order in the atomic displacements, our self-energy does not include the standard Debye-Waller (DW) contribution [33,46], and this term must be added separately to be consistent with previous work. To evaluate this contribution, we use the method presented in Ref. [104] as implemented in the PHonon package on a coarse Brillouin-zone mesh, and add the result to the FM self-energy before proceeding with the interpolation procedure described above. The dispersions of the Fan-Migdal and Debye-Waller self-energies for the valence and conduction bands of LiF are shown in Ref. [47].

In Figs. 8(c) and 8(d) we analyze the convergence of the Fan-Migdal and Debye-Waller contributions to the polaron energy with the Brillouin-zone grid for the electron and the hole polaron, respectively. As we discuss in Ref. [47], in the case of the large electron polaron the quasiparticle amplitudes are localized around the conduction band bottom, so that relatively dense $\mathbf{k}$ meshes are needed to converge the average of the FM+DW self-energy within 1 meV. In contrast, in the case of the small hole polaron, the quasiparticle amplitudes are distributed across the entire Brillouin zone, so that coarser meshes are sufficient to achieve convergence. The converged values for the FM+DW self-energy contribution to the polaron eigenvalue are -0.35 and 0.30 eV for the electron and the hole polaron, respectively.

By combining the above contributions, we find formation energies of -0.60 and -2.20 eV for the electron and the hole polaron, respectively. Note that the formation energy for the hole polaron is negative, but the associated renormalization of the ionization energy and thus of the band gap is positive. This brings the total polaronic renormalization of the band gap to -2.8 eV. This value is considerably larger than that obtained within the Allen-Heine theory (-1.2 eV), where the Fan-Migdal and Debye-Waller self-energies are evaluated at the band edges, without taking into account the quasiparticle amplitudes. This result demonstrates that polaronic localization can have a significant effect on the band-gap renormalization of solids. We elaborate more on this point in the companion paper [47].

VI. LOCALIZATION AND TRANSLATIONAL INVARIANCE

For completeness, in this final section we address one formal question that arises in the polaron literature, and which pertains to the nature of the localization of a polaron in real space [81,84,85].

The question is on how to reconcile the spatial localization of the polaron with the translational invariance of the Hamiltonian in Eq. (1): Since $\hat{H}$ commutes with the the lattice translation operator, the ground state must also be an eigenstate of the translation. This issue has already been discussed in prior literature [81], therefore, we only touch upon those aspects that are relevant to this work.

To clarify the relation between translational invariance and localization, we use the textbook example of the hydrogen atom as a proxy for an interacting electron-phonon system. In this proxy, the proton replaces the concentration of ionic charge resulting from the formation of the polaron. The general expression for the eigenfunction of the hydrogen atom Hamiltonian [107] is

$$\Psi_{\mathbf{k}}(\mathbf{r}_e, \mathbf{r}_p) = \frac{1}{\sqrt{V}} \exp\left[i\mathbf{k} \cdot \frac{m_e \mathbf{r}_e + m_p \mathbf{r}_p}{m_e + m_p} \right] \psi_{nlm}(\mathbf{r}_e - \mathbf{r}_p), \tag{80}$$

where $\mathbf{r}_e$ and $\mathbf{r}_p$ are the position of the electron and the proton, respectively, m_e and m_p their respective masses, ψ_{nlm} is the hydrogenic eigenstate in the standard notation, and V is the volume of the box where the atom is contained. Since the Hamiltonian of this atom commutes with the translation operator $\hat{T}_{\mathbf{R}}$ that acts simultaneously on $\mathbf{r}_e$ and $\mathbf{r}_p$, $\Psi_{\mathbf{k}}$ is also
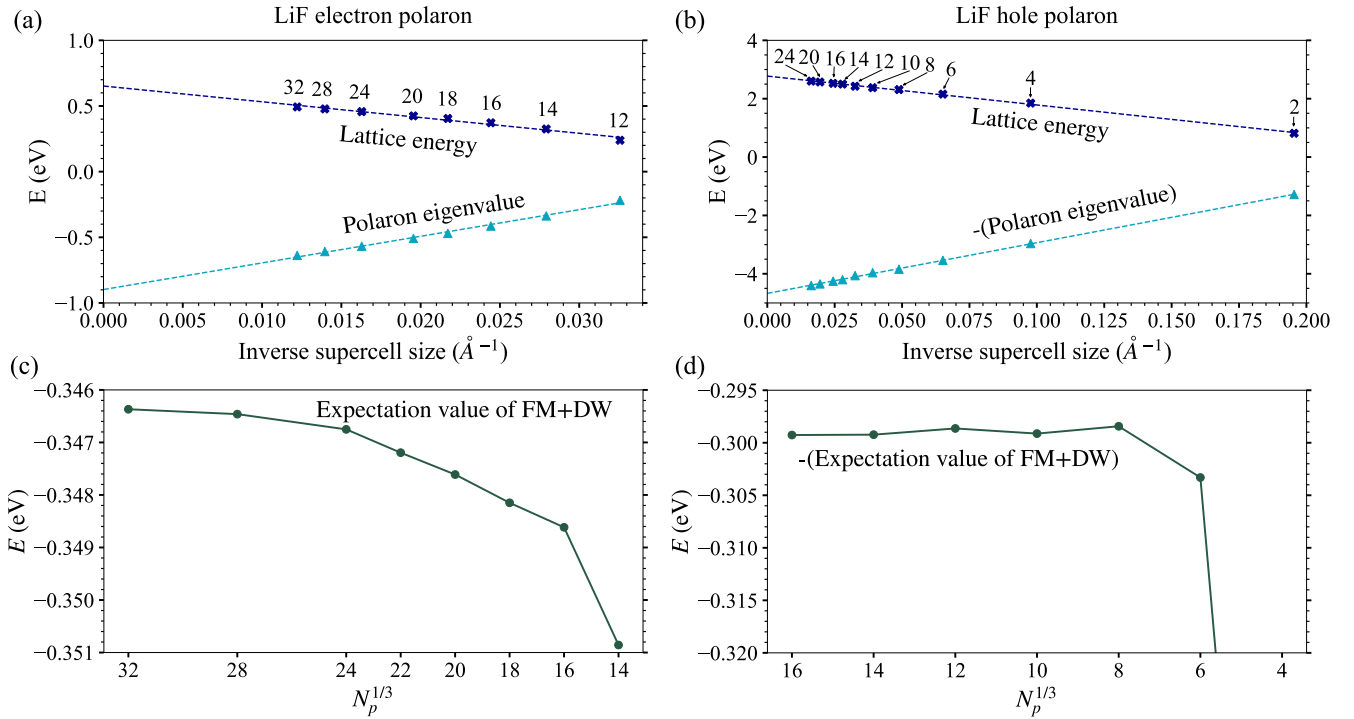
FIG. 8. Analysis of the various contributions to the polaron formation energy in the lowest-order approximation, Eqs. (58), (62), and (63). (a) Polaron eigenvalue (light blue triangles) and lattice energy (dark blue crosses) as a function of the supercell size for the electron polaron in LiF. The supercell size is given as L^{-1}, where L^3 is the supercell volume. The numbers next to the data points indicate the number of unit cells in each direction of the homogeneous Born–von Karman supercell or, equivalently, the number of **k** points in each direction of the homogeneous mesh of the Brillouin zone. The dashed lines correspond to the extrapolation of each contribution to the infinite supercell size. (b) Same as (a) but for the hole polaron in LiF. (c) Expectation value of the FM+DW self-energy over the polaron quasiparticle amplitudes for the electron polaron in LiF, as a function of the number of **k** points in each direction of the homogeneous mesh of the Brillouin zone. (d) Same as (c) but for the hole polaron in LiF.

a translation eigenstate:

$$\hat{T}_{\mathbf{R}}\Psi_{\mathbf{k}}(\mathbf{r}_e, \mathbf{r}_p) = \exp(-i\mathbf{k}\cdot\mathbf{R})\,\Psi_{\mathbf{k}}(\mathbf{r}_e, \mathbf{r}_p), \quad (81)$$

as well as an eigenstate of the total momentum with eigenvalue $\hbar\mathbf{k}$. From these relations we see that the coupled electron-proton state is completely delocalized. In particular, if we look for the probability $n(\mathbf{r}_e)$ of finding the electron irrespective of the location of the proton, we have

$$n(\mathbf{r}_e) = \int d\mathbf{r}_p|\Psi_{\mathbf{k}}(\mathbf{r}_e, \mathbf{r}_p)|^2 = \frac{1}{V}, \quad (82)$$

therefore, the electron is fully delocalized over the box that contains the atom. On the other hand, if we consider the conditional probability $P(\mathbf{r}_e|\mathbf{r}_p = \mathbf{r}_0)$ of finding the electron when the proton is located at $\mathbf{r}_0$, we find

$$P(\mathbf{r}_e|\mathbf{r}_p = \mathbf{r}_0) = |\Psi_{\mathbf{k}}(\mathbf{r}_e, \mathbf{r}_0)|^2 = \frac{1}{V}|\psi_{nlm}(\mathbf{r}_e - \mathbf{r}_0)|^2, \quad (83)$$

which is localized around $\mathbf{r}_0$. Similar considerations hold for excitons within the Bethe-Salpeter formalism [53]. The situation for polarons is analogous to the above example of the hydrogen atom: electrons and atomic displacements are localized with respect to each other, but the many-body wave function is delocalized in the sense of Eq. (81).

In the same way as it is convenient to study the hydrogen atom by using a center-of-mass reference frame, or equivalently by "pinning" the center of mass at the origin of the reference frame, in our approach we pin the polaron at a fixed location in space. In Sec. V A this is implicitly achieved by centering the variational ansatz at $\mathbf{r} = 0$ [cf. Eq. (72)], and in Sec. V B it is achieved by initializing the polaron wave function using a wave packet at the center of the BvK supercell.

The use of polaron pinning is not mere technical expedient, it is rather a necessity. Indeed, one limitation of the single-particle Green's function G is that it only contains electronic variables, therefore, the Dyson orbitals $f_s(\mathbf{r})$ appearing in Eq. (34) only depend on the electronic coordinates, unlike many-body wave functions such as the one in Eq. (80).

There are several possible avenues to overcome this limitation: (i) One could abandon the standard single-particle Green's function formalism, and replace it with Green's functions for both electrons and phonons. This choice carries two limitations: first, the complexity of these Green's functions grows combinatorially with the number of phonon modes; second, this choice would defeat our purpose of developing a unifying formalism that connects polaron calculations and many-body calculations of band-structure renormalization. (ii) One could work directly with many-body wave functions of electrons and phonons. This is essentially the approach taken by Pekar and coworkers in Refs. [84,85], and is amenable to incorporating translational invariance. The drawback of this approach is that it is a wave-function method, hence, it faces the same exponential wall that hinders direct

solutions of the many-body Schrödinger equation for interacting electrons. (iii) One could formally break the translational invariance of the Hamiltonian in Eq. (1) by introducing a small perturbation. Such a perturbation could be the potential of an impurity or the confining potential of a finite crystal.

In the latter case (iii), the electron and the lattice distortion are pinned, and the symmetry-breaking perturbation can be set to zero at the end of the calculation. This approach is equivalent to retaining small but nonzero fictitious forces in Schwinger's functional derivation, Eq. (8). In this work, when we refer to polaron localization in real space, we implicitly consider that such a small perturbation is present in the Hamiltonian as an additional term in Eq. (1), so that translational invariance is slightly broken, localization survives, and the energetics of the polaron is not affected.

VII. SUMMARY AND OUTLOOK

In summary, we have presented an *ab initio* Green's function theory of polarons, which unifies the perturbative weak-coupling approach and the adiabatic strong-coupling approach to the polaron problem. Starting from a general electron-phonon Hamiltonian, we have derived a Dyson equation for the electron Green's function, accounting for possible static displacements of the atomic nuclei in the ground state of the system with an excess electron or hole. In addition to the conventional Fan-Midgal dynamical self-energy, we identified a self-energy contribution which results from static lattice distortions in the polaron state. After presenting the general formalism, we have outlined several approximations that enable practical implementations of the theory in current *ab initio* software. This analysis establishes unambiguously the links between our formalism, density functional calculations of polarons [34,35], and the Allen-Heine theory of band-structure renormalization [46].

In order to benchmark our method, we have studied the ground-state energy of the Fröhlich polaron, and found that our approach is in very good agreement with Feynman's path-integral solution and with diagrammatic Monte Carlo calculations, at all coupling strengths. As a first *ab initio* calculation using this method, we have computed the polaronic band-gap renormalization in LiF. The main results and implications of our *ab initio* calculations are discussed in the companion paper [47].

The agreement between our theory and previous diagrammatic Monte Carlo calculations for the Fröhlich model might appear surprising. In fact, these previous calculations involve summations over a very large number of electron-phonon self-energy diagrams [28,29,93], while only two self-energies are considered in this work. The main difference between our approach and the diagrammatic Monte Carlo method is that in our case the sum over all electron-phonon diagrams is replaced by a set of self-consistent equations defining the exact interacting Green's function. This strategy allows us to describe localization effects, which become dominant at strong coupling, via the self-consistent polaronic self-energy given in Eq. (33). The remaining nonadiabatic electron-phonon interactions are encoded in the FM self-energy given in Eq. (18), whose lowest-order approximation is enough to capture the

renormalization of large polarons at weak coupling. Higher-order diagrams could be included via the vertex function Γ, but on the basis of the results presented in this work we expect their contribution to be small. It is possible that the inclusion of vertex corrections will further reduce the slight deviation between our present results and diagrammatic Monte Carlo calculations.

The success of our self-consistent many-body approach is reminiscent of Hedin's *GW* equations for the electron-electron problem [56,76]. By converting the infinite sum of diagrams for the bare Coulomb interaction into a set of self-consistent equations, it was found that the electron-electron self-energy could be expanded in terms of the screened Coulomb interaction, and this strategy proved highly successful over the past four decades [48,53–55]. In the same spirit, in this work we employed the functional derivative technique of Schwinger to replace a summation over infinite electron-phonon diagrams into the self-consistent solution of a set of equations for the electron Green's function and the interaction self-energies. This strategy allowed us to show that adiabatic localization and dynamical many-body effects are not separate and inconsistent ways to look at the electron-phonon problem. Rather, both contributions are a complementary aspect of the same problem, and need to be taken into account on the same footing.

Many improvements upon the present method are possible. For example, in this work we mostly focused on perturbative solutions of the self-consistent many-body polaron equations; in the future it will be interesting to test full-blown self-consistent schemes for better accuracy. Furthermore, in this work we only focus on the polaron ground state, but the formalism contains information about excited states as well; work on polaron excitations would be useful to investigate finite-temperature properties and the response of polarons to external fields. Another interesting development would be to calculate the renormalization of the phonon Green's function on the same footing as the electron Green's function, which would require upgrading the starting point in Eq. (1) to a more general electron-ion Hamiltonian [33,108]. This further step would allow us to investigate the signature of polarons in vibrational spectroscopy via the change in the phonon frequencies [109]. Lastly, systematic calculations using the present approach for a broad library of materials will be needed to assess the significance of polaronic effects, and their role in the phonon-induced renormalization of the band structure of solids.

We hope that this work will be useful as a starting point to investigate polarons in real materials from the point of view of *ab initio* many-body methods.

ACKNOWLEDGMENTS

[1] A. S. Alexandrov and N. F. Mott, *Polarons and Bipolarons* (World Scientific, Singapore, 1996).

[2] A. S. Alexandrov, *Polarons in Advanced Materials*, Springer Series in Materials Science, Vol. 103 (Springer, Dordrecht, 2007).

[3] D. Emin, *Polarons* (Cambridge University Press, Cambridge, 2012).

[4] J. T. Devreese, arXiv:1611.06122.

[5] L. D. Landau, Phys. Z. Sowjetunion **3**, 664 (1933).

[6] S. Pekar, Zh. Eksp. Teor. Fiz. **16**, 341 (1946).

[7] C. Franchini, M. Reticcioli, M. Setvin, and U. Diebold, Nat. Rev. Mater. **6**, 560 (2021).

[8] G.-m. Zhao, M. B. Hunt, H. Keller, and K. A. Müller, Nature (London) **385**, 236 (1997).

[9] J. M. D. Teresa, M. R. Ibarra, P. A. Algarabel, C. Ritter, C. Marquina, J. Blasco, J. García, A. del Moral, and Z. Arnold, Nature (London) **386**, 256 (1997).

[10] K. Miyata, D. Meggiolaro, M. T. Trinh, P. P. Joshi, E. Mosconi, S. C. Jones, F. De Angelis, and X.-Y. Zhu, Sci. Adv. **3** (2017).

[11] S. Moser, L. Moreschini, J. Jaćimović, O. S. Barišić, H. Berger, A. Magrez, Y. J. Chang, K. S. Kim, A. Bostwick, E. Rotenberg, L. Forró, and M. Grioni, Phys. Rev. Lett. **110**, 196403 (2013).

[12] C. Chen, J. Avila, E. Frantzeskakis, A. Levy, and M. C. Asensio, Nat. Commun. **6**, 8585 (2015).

[13] Z. Wang, S. McKeown Walker, A. Tamai, Y. Wang, Z. Ristic, F. Y. Bruno, A. de la Torre, S. Riccò, N. C. Plumb, M. Shi, P. Hlawenka, J. Sánchez-Barriga, A. Varykhalov, T. K. Kim, M. Hoesch, P. D. C. King, W. Meevasana, U. Diebold, J. Mesot, B. Moritz *et al.*, Nat. Mater. **15**, 835 (2016).

[14] C. Cancellieri, A. S. Mishchenko, U. Aschauer, A. Filippetti, C. Faber, O. S. Barišić, V. A. Rogalev, T. Schmitt, N. Nagaosa, and V. N. Strocov, Nat. Commun. **7**, 10386 (2016).

[15] C. Verdi, F. Caruso, and F. Giustino, Nat. Commun. **8**, 15769 (2017).

[16] J. M. Riley, F. Caruso, C. Verdi, L. B. Duffy, M. D. Watson, L. Bawden, K. Volckaert, G. van der Laan, T. Hesjedal, M. Hoesch, F. Giustino, and P. D. C. King, Nat. Commun. **9**, 2305 (2018).

[17] S. X. Zhang, D. C. Kundaliya, W. Yu, S. Dhar, S. Y. Young, L. G. Salamanca-Riba, S. B. Ogale, R. D. Vispute, and T. Venkatesan, J. Appl. Phys. **102**, 013701 (2007).

[18] J. L. M. van Mechelen, D. van der Marel, C. Grimaldi, A. B. Kuzmenko, N. P. Armitage, N. Reyren, H. Hagemann, and I. I. Mazin, Phys. Rev. Lett. **100**, 226403 (2008).

[19] M. Reticcioli, I. Sokolović, M. Schmid, U. Diebold, M. Setvin, and C. Franchini, Phys. Rev. Lett. **122**, 016805 (2019).

[20] H. Fröhlich, H. Pelzer, and S. Zienau, London, Edinburgh Dublin Philos. Mag. J. Sci. **41**, 221 (1950).

[21] H. Fröhlich, Adv. Phys. **3**, 325 (1954).

[22] T. Holstein, Ann. Phys. **8**, 325 (1959).

[23] T. Holstein, Ann. Phys. **8**, 343 (1959).

[24] W. P. Su, J. R. Schrieffer, and A. J. Heeger, Phys. Rev. Lett. **42**, 1698 (1979).

[25] A. S. Alexandrov and J. T. Devreese, *Advances in Polaron Physics*, Springer Series in Solid-State Sciences (Springer, Berlin, 2010), Vol. 159.

[26] R. P. Feynman, Phys. Rev. **97**, 660 (1955).

[27] Y. Ōsaka, Prog. Theor. Phys. **22**, 437 (1959).

[28] N. V. Prokof'ev and B. V. Svistunov, Phys. Rev. Lett. **81**, 2514 (1998).

[29] A. S. Mishchenko, N. V. Prokof'ev, A. Sakamoto, and B. V. Svistunov, Phys. Rev. B **62**, 6317 (2000).

[30] S. Ciuchi, F. de Pasquale, S. Fratini, and D. Feinberg, Phys. Rev. B **56**, 4494 (1997).

[31] S. Fratini and S. Ciuchi, Phys. Rev. Lett. **91**, 256403 (2003).

[32] F. Grusdt, Phys. Rev. B **93**, 144302 (2016).

[33] F. Giustino, Rev. Mod. Phys. **89**, 015003 (2017).

[34] W. H. Sio, C. Verdi, S. Poncé, and F. Giustino, Phys. Rev. Lett. **122**, 246403 (2019).

[35] W. H. Sio, C. Verdi, S. Poncé, and F. Giustino, Phys. Rev. B **99**, 235139 (2019).

[36] N.-E. Lee, H.-Y. Chen, J.-J. Zhou, and M. Bernardi, Phys. Rev. Materials **5**, 063805 (2021).

[37] P. Garcia-Goiricelaya, J. Lafuente-Bartolome, I. G. Gurtubay, and A. Eiguren, Commun. Phys. **2**, 81 (2019).

[38] C. Franchini, G. Kresse, and R. Podloucky, Phys. Rev. Lett. **102**, 256402 (2009).

[39] N. A. Deskins and M. Dupuis, Phys. Rev. B **75**, 195212 (2007).

[40] S. Lany and A. Zunger, Phys. Rev. B **80**, 085202 (2009).

[41] J. B. Varley, A. Janotti, C. Franchini, and C. G. Van de Walle, Phys. Rev. B **85**, 081109(R) (2012).

[42] M. Setvin, C. Franchini, X. Hao, M. Schmid, A. Janotti, M. Kaltak, C. G. Van de Walle, G. Kresse, and U. Diebold, Phys. Rev. Lett. **113**, 086402 (2014).

[43] B. Himmetoglu, A. Janotti, L. Bjaalie, and C. G. Van de Walle, Phys. Rev. B **90**, 161102(R) (2014).

[44] S. Kokott, S. V. Levchenko, P. Rinke, and M. Scheffler, New J. Phys. **20**, 033023 (2018).

[45] M. Reticcioli, M. Setvin, X. Hao, P. Flauger, G. Kresse, M. Schmid, U. Diebold, and C. Franchini, Phys. Rev. X **7**, 031053 (2017).

[46] P. B. Allen and V. Heine, J. Phys. C: Solid State Phys. **9**, 2305 (1976).

[47] J. Lafuente-Bartolome, C. Lian, W. H. Sio, I. G. Gurtubay, A. Eiguren, and F. Giustino, Phys. Rev. Lett. **129**, 076402 (2022)..

[48] M. S. Hybertsen and S. G. Louie, Phys. Rev. B **34**, 5390 (1986).

[49] S. Baroni, S. de Gironcoli, A. Dal Corso, and P. Giannozzi, Rev. Mod. Phys. **73**, 515 (2001).

[50] A. Fetter and J. Walecka, *Quantum Theory of Many-Particle Systems* (Dover, New York, 2003).

[51] J. Schwinger, Proc. Natl. Acad. Sci. USA **37**, 452 (1951).

[52] T. Kato, T. Kobayashi, and M. Namiki, Prog. Theor. Phys. Suppl. **15**, 3 (1960).

[53] G. Onida, L. Reining, and A. Rubio, Rev. Mod. Phys. **74**, 601 (2002).

[54] L. Reining, WIREs Comput. Mol. Sci. **8**, e1344 (2018).

[55] D. Golze, M. Dvorak, and P. Rinke, Front. Chem. **7**, 377 (2019).

[56] L. Hedin and S. Lundqvist, *Effects of Electron-Electron and Electron-Phonon Interactions on the One-Electron States of Solids*, edited by F. Seitz, D. Turnbull, and H. Ehrenreich, Solid State Physics (Academic, New York, 1969), Vol. 23.

[57] S. Engelsberg and J. R. Schrieffer, Phys. Rev. **131**, 993 (1963).

[58] L. P. Kadanoff and G. Baym, *Quantum Statistical Mechanics: Green's Function Methods in Equilibrium and Nonequilibrium Problems*, Frontiers in Physics (Benjamin, New York, 1962).

[59] M. Kang, S. W. Jung, W. J. Shin, Y. Sohn, S. H. Ryu, T. K. Kim, M. Hoesch, and K. S. Kim, Nat. Mater. **17**, 676 (2018).

[60] A. Eiguren, C. Ambrosch-Draxl, and P. M. Echenique, Phys. Rev. B **79**, 245103 (2009).

[61] P. B. Allen, Phys. Rev. B **18**, 5217 (1978).

[62] A. Marini, Phys. Rev. Lett. **101**, 106405 (2008).

[63] F. Giustino, S. G. Louie, and M. L. Cohen, Phys. Rev. Lett. **105**, 265501 (2010).

[64] X. Gonze, P. Boulanger, and M. Côté, Ann. Phys. **523**, 168 (2011).

[65] S. Poncé, Y. Gillet, J. Laflamme Janssen, A. Marini, M. Verstraete, and X. Gonze, J. Chem. Phys. **143**, 102813 (2015).

[66] J. P. Nery and P. B. Allen, Phys. Rev. B **94**, 115135 (2016).

[67] F. Caruso, M. Troppenz, S. Rigamonti, and C. Draxl, Phys. Rev. B **99**, 081104(R) (2019).

[68] F. Brown-Altvater, G. Antonius, T. Rangel, M. Giantomassi, C. Draxl, X. Gonze, S. G. Louie, and J. B. Neaton, Phys. Rev. B **101**, 165102 (2020).

[69] A. Miglio, V. Brousseau-Couture, E. Godbout, G. Antonius, Y.-H. Chan, S. G. Louie, M. Côté, M. Giantomassi, and X. Gonze, npj Comput. Mater. **6**, 167 (2020).

[70] A. Marini, S. Poncé, and X. Gonze, Phys. Rev. B **91**, 224310 (2015).

[71] M. Zacharias and F. Giustino, Phys. Rev. B **94**, 075125 (2016).

[72] M. Zacharias and F. Giustino, Phys. Rev. Research **2**, 013357 (2020).

[73] O. V. Konstantinov and V. I. Perel, Zh. Eksp. Teor. Fiz. **39**, 197 (1960) [Sov. Phys.–JETP **12**, 142 (1961)].

[74] G. Stefanucci and R. van Leeuwen, *Nonequilibrium Many-Body Theory of Quantum Systems: A Modern Introduction* (Cambridge University Press, Cambridge, 2013).

[75] R. D. Mattuck, *A Guide to Feynman Diagrams in the Many-body Problem* (Dover, New York, 1992).

[76] L. Hedin, Phys. Rev. **139**, A796 (1965).

[77] A. B. Migdal, Zh. Eksp. Teor. Fiz. **34**, 1438 (1958) [Sov.–Phys. JETP **7**, 996 (1958)].

[78] G. Grimvall, *The Electron-phonon Interaction in Metals* (North-Holland, Amsterdam, 1981).

[79] V. M. Galitskii and A. B. Migdal, Zh. Eksp. Teor. Fiz. **34**, 139 (1957) [Sov. Phys.–JETP **7**, 96 (1958)].

[80] B. Holm and F. Aryasetiawan, Phys. Rev. B **62**, 4858 (2000).

[81] G. Allcock, Adv. Phys. **5**, 412 (1956).

[82] G. Höhler, Z. Naturforschg. **9**, 801 (1954).

[83] N. N. Bogolyubov and A. V. Soldatov, Moscow Univ. Phys. **71**, 356 (2016).

[84] V. M. Buimistrov and S. I. Pekar, Zh. Eksp. Teor. Fiz. **32**, 1193 (1957) [Sov. Phys.–JETP **5**, 970 (1957)].

[85] V. M. Buimistrov and S. I. Pekar, Zh. Eksp. Teor. Fiz. **33**, 1271 (1957) [Sov. Phys.–JETP **6**, 977 (1957)].

[86] F. A. Berezin, *The Method of Second Quantization* (Nauka, Moscow, 1986).

[87] T. D. Lee, F. E. Low, and D. Pines, Phys. Rev. **90**, 297 (1953).

[88] C. Verdi and F. Giustino, Phys. Rev. Lett. **115**, 176401 (2015).

[89] N. Kandolf, C. Verdi, and F. Giustino, Phys. Rev. B **105**, 085148 (2022).

[90] G. D. Mahan, *Many-Particle Physics*, 2nd ed. (Plenum, New York, 1993).

[91] T. D. Schultz, Phys. Rev. **116**, 526 (1959).

[92] R. Rosenfelder and A. Schreiber, Phys. Lett. A **284**, 63 (2001).

[93] T. Hahn, S. Klimin, J. Tempere, J. T. Devreese, and C. Franchini, Phys. Rev. B **97**, 134305 (2018).

[94] S. J. Miyake, J. Phys. Soc. Jpn. **38**, 181 (1975).

[95] P. Giannozzi Jr, O. Andreussi, T. Brumme, O. Bunau, M. B. Nardelli, M. Calandra, R. Car, C. Cavazzoni, D. Ceresoli, M. Cococcioni, N. Colonna, I. Carnimeo, A. D. Corso, S. de Gironcoli, P. Delugas, R. A. D. Jr, A. Ferretti, A. Floris, G. Fratesi, G. Fugallo *et al.*, J. Phys.: Condens. Matter **29**, 465901 (2017).

[96] J. P. Perdew, K. Burke, and M. Ernzerhof, Phys. Rev. Lett. **77**, 3865 (1996).

[97] D. R. Hamann, Phys. Rev. B **88**, 085117 (2013).

[98] M. van Setten, M. Giantomassi, E. Bousquet, M. Verstraete, D. Hamann, X. Gonze, and G.-M. Rignanese, Comput. Phys. Commun. **226**, 39 (2018).

[99] N. Marzari and D. Vanderbilt, Phys. Rev. B **56**, 12847 (1997).

[100] I. Souza, N. Marzari, and D. Vanderbilt, Phys. Rev. B **65**, 035109 (2001).

[101] F. Giustino, M. L. Cohen, and S. G. Louie, Phys. Rev. B **76**, 165108 (2007).

[102] G. Pizzi, V. Vitale, R. Arita, S. Blügel, F. Freimuth, G. Géranton, M. Gibertini, D. Gresch, C. Johnson, T. Koretsune, J. Ibañez-Azpiroz, H. Lee, J.-M. Lihm, D. Marchand, A. Marrazzo, Y. Mokrousov, J. I. Mustafa, Y. Nohara, Y. Nomura, L. Paulatto *et al.*, J. Phys.: Condens. Matter **32**, 165902 (2020).

[103] S. Poncé, E. Margine, C. Verdi, and F. Giustino, Comput. Phys. Commun. **209**, 116 (2016).

[104] J.-M. Lihm and C.-H. Park, Phys. Rev. B **101**, 121102(R) (2020).

[105] J. Heyd, G. E. Scuseria, and M. Ernzerhof, J. Chem. Phys. **118**, 8207 (2003).

[106] D. R. Hamann and D. Vanderbilt, Phys. Rev. B **79**, 045109 (2009).

[107] E. Merzbacher, *Quantum Mechanics* (Wiley, New York, 1998).

[108] G. Baym, Ann. Phys. **14**, 1 (1961).

[109] S. J. Miyake, J. Phys. Soc. Jpn. **41**, 747 (1976).

[110] http://www.tacc.utexas.edu.

Correction: The previously published first sentence of the Acknowledgment section contained errors and has been fixed.